Measurement of alkyl and multifunctional organic nitrates by proton-transfer-reaction mass spectrometry

Marius Duncianu, Marc David, Sakthivel Kartigueyane, Manuela Cirtog, Jean-François Doussin, Benedicte Picquet-Varrault

Atmos. Meas. Tech., 10, 1445–1463, 2017
www.atmos-meas-tech.net/10/1445/2017/
doi:10.5194/amt-10-1445-2017

Atmospheric Measurement Techniques
Open Access
EGU

Measurement of alkyl and multifunctional organic nitrates by proton-transfer-reaction mass spectrometry

Marius Duncianu, Marc David, Sakthivel Kartigueyane, Manuela Cirtog, Jean-François Doussin, and Benedicte Picquet-Varrault

Laboratoire Interuniversitaire des Systèmes Atmosphériques (LISA), UMR-CNRS 7583, Université Paris-Est-Créteil (UPEC) et Université Paris Diderot (UPD), Paris, France

Correspondence to: Benedicte Picquet-Varrault (benedicte.picquet-varrault@lisa.u-pec.fr)

Received: 5 October 2016 – Discussion started: 7 November 2016
Revised: 31 January 2017 – Accepted: 2 March 2017 – Published: 18 April 2017

Abstract. A commercial PTR-TOF-MS has been optimized in order to allow the measurement of individual organic nitrates in the atmosphere. This has been accomplished by shifting the distribution between different ionizing analytes, $H_3O^+ / H_3O^+(H_2O)_n$ or NO^+ / NO_2^+. The proposed approach has been proven to be appropriate for the online detection of individual alkyl nitrates and functionalized nitrates. It has been shown that hydroxyl and ketonitrates have a high affinity towards NO^+, leading to the formation of an adduct that allows the easy identification of the organic nitrate (R) from the R–NO^+ ion signal. The recorded sensitivities for both ionization modes correspond to detection limits of tens of ppt min^{-1} in the case of hydroxy- and ketonitrates. Alkyl nitrates exhibit a moderate affinity towards NO^+ ionization leading to detection units of few hundreds of ppt and the highest sensitivity in H_3O^+ mode was obtained for the water adducts signals. However, this method exhibits much lower capabilities for the detection of peroxyacetyl nitrates with detection limits in the ppb range.

1 Introduction

Organic nitrates are an important species of the reactive nitrogen (NO_y) budget in the troposphere. They are formed in NO_x rich air by the degradation of hydrocarbons initiated by OH (daytime) and NO_3 (nighttime) radicals. Since organic nitrates have lifetimes of several days or weeks (Perring et al., 2010), they can act as reservoirs for reactive nitrogen by undergoing long-range transport in the free troposphere before decomposing and releasing NO_x. They therefore play a key role in the ozone formation as they sequester reactive nitrogen in rich NO_x regions and release it in regions where production of ozone may be NO_x limited. The significant impact of organic nitrate chemistry on the ozone budget has been confirmed by recent modeling studies (Curci et al., 2009; Horowitz et al., 2007).

In addition, several field studies have shown that both polluted and remote atmospheres contain a large variety of organic nitrates, which significantly affects the NO_y budget (for example, 35–40 % as reported by Buhr et al., 1990, and up to 70 % according to a modeling study performed by Madronich and Calvert, 1990). They are not only monofunctional alkyl nitrates and peroxyacetyl nitrates (PANs) but also multifunctional alkyl nitrates (Browne et al., 2013; Fischer et al., 2000; Kastler and Ballschmiter, 1999; Muthuramu et al., 1993; O'Brien et al., 1995). The latter include (i) hydroxynitrates formed by the OH oxidation of alkenes followed by isomerization processes of alkoxy radicals (Arey et al., 2001), (ii) carbonyl nitrates which are produced by the NO_3 oxidation of alkenes (Berndt and Böge, 1995) and also as second-generation oxidation products of hydrocarbons and (iii) dinitrates which are also expected to be second-generation oxidation products (Atkinson, 2000; Barnes et al., 1990; Roberts, 1990).

However, measurements of organic nitrates during field campaigns remain rare, thus preventing a precise evaluation of their impact on the NO_y budget in a wide variety of environments. The main problems in analyzing organic nitrates in the atmosphere are, first, the great complexity of the mixtures due to the huge number of precursors and formation pathways and, second, the fact that organic nitrates are ex-

plosive compounds and only few of them are commercially available. So standards have to be synthesized. These analytical difficulties also affect our capability to study the chemical processes in which organic nitrates are involved during lab experiments (e.g., in simulation chambers).

Table 1 summarizes, without the intent of being exhaustive, some keystone articles concerning the organic nitrates analysis in field and laboratory studies.

Two approaches have been applied for the analysis of complex mixtures of organic nitrates during field and lab experiments. The first is analysis at the molecular scale, which is a powerful approach to elucidate mechanisms but has the drawback to be often limited to a low number of species, followed by functional group analysis, which is very useful to assess global budgets but brings little information about the understanding of processes. The second approach allows us to shortcut the complexity of the organic nitrates chemistry governing their production, transformation and removal processes and assess directly the sum of peroxynitrates ΣAN and alkyl nitrates ΣAN (Day et al., 2002; Perring et al., 2010). The thermal dissociation (TD) properties of different classes of nitrates were used as an analytical tool to probe the global chemistry of $RONO_2$, utilizing laser-induced florescence (LIF), cavity ring down spectroscopy (CRDS) (Paul et al., 2009) or cavity attenuated phase shift (CAPS) (Sadanaga et al., 2016) to quantify the NO_2 evolved from the organic nitrates decomposition. In a similar way, the infrared spectroscopy (IR) was used to monitor the time-dependent loss of organic nitrates and measure the rate of homolytic O−N bond cleavage (Francisco and Krylowski, 2005) by employing specific absorption bands in IR ($1638\,cm^{-1}$). Although notoriously powerful analytical techniques, the LIF, CRDS, CAPS and IR exhibit poor capabilities in the individual quantification of organic nitrates mixtures due to their intrinsic conceptual operation mode.

Historically, measurements of individual organic nitrates have been conducted by gas chromatography coupled to electron capture detection (GC/ECD), both coupled or not (Atlas, 1988; Blake et al., 1999; Flocke et al., 2005; Fukui and Doskey, 1998; Muthuramu et al., 1993) to a pyrolysis/luminol chemiluminescence (CL) detector (Buhr et al., 1990; Fischer et al., 2000; Flocke et al., 1991; Gaffney et al., 1999; Hao et al., 1994; Winer et al., 1974), to electron impact mass spectrometry (EI-MS) (Luxenhofer and Ballschmiter, 1994; Luxenhofer et al., 1994) or to negative ion chemical ionization mass spectrometry (NI/CIMS) (Beaver et al., 2012; Tanimoto et al., 1999) using thermal electrons (e_{th}^-). Abundant in marine environments, the halocarbons are highly sensitive towards the ECD detection (Fischer et al., 2002, 2000) and may generate artifacts in the organic nitrates identification and quantification (Fukui and Doskey, 1998).

Although the chromatographic separation represents an effective analytical tool, the organic nitrate identification relies mainly on the retention times, while the dedicated detectors are only able to confirm, in the best case scenario, the presence of the nitrate functional group in the molecule. Illustrative examples are given by the studies of Luxenhofer et al. (1994) and Kastler and Ballschmiter (1999), who succeed to analyze complex mixtures of alkyl and multifunctional organic nitrates by combining separation with liquid and gas chromatography and detection using the intense mass-to-charge (m/z) 46 fragment ion that corresponds to NO_2^+. The same study highlights possible interferences with dinitrophenols, nitro- and dinitrocresols, pentachloronitrobenzene and to a smaller extent nitrophenols.

Besides the poor temporal resolution, another major drawback of this method is represented by the recovery factor decline with longer times in the chromatographic columns. According to Roberts et al. (2002), the sensitivity of this method for PANs is characterized by a diminishing response factor proportional to the compounds retention time through the column. Measurement of functionalized (oxygenated) nitrates appears to be a greater challenge as the lower vapor pressures and stronger surface interactions of these molecules make sampling and chromatographic techniques less appropriate. Additionally, the detection of functionalized nitrates by electron impact mass spectrometry has proven to be difficult, mainly due to the instability and thus the fragmentation of the molecular ion formed (Mills et al., 2016; Roberts, 1990; Rollins et al., 2010).

Lately, the newly developed capabilities in atmospheric pressure/chemical ionization mass spectrometry (AP-CIMS) (Huey, 2007; Perraud et al., 2010; Slusher et al., 2004; Teng et al., 2015) prove to be potentially powerful tools in organic nitrates analysis. Several types of CIMS have been highlighted by the literature, and the technique is currently one of the most promising analytic tools.

The AP-CIMS uses methanol as a proton source in order to generate RH^+ peaks of the parent ions. Therefore the nitrogen-containing ions are characterized by even m/z ratios, while the analytes containing only C, H and O appear at odd m/z. Several PANs were identified as gas-phase products of the α-pinene + NO_3 reaction with this technique (Perraud et al., 2010). The protonated molecular ions were identified and the most intense fragments in the MS/MS scan corresponds to losses of NO_2, HNO_3 and to a smaller extent $HOONO_2$. Hydroxynitrates and ketonitrates have also been detected with this technique. For hydroxynitrates, RH^+ peaks as well as fragments corresponding to the losses of H_2O and $NO_2 + H_2O$ in the MS/MS mode were detected (Perraud et al., 2010; Schoon et al., 2007; Tuazon et al., 1999).

The thermal dissociation–chemical ionization mass spectrometry (TD-CIMS) technique has been used for measurement of PANs and other multifunctional organic nitrates by the means of I^- reaction (Lee et al., 2014; Slusher et al., 2004; Xiong et al., 2015). The obtained carboxylate ion is unique for each parent species, and the only significant interference that has been identified is at ppb levels of NO

Table 1. Summarized analytical approaches into the organic nitrate analysis.

Type of study	Analytes	DL/time or normalized sensitivity	Ionizing species	Experimental setup	Study
Synthesis	PAN	< 40 ppb	O_3+NO KOH / O_3+NO	CL NO_x IC KOH / CL NO_x	Winer et al. (1974), Grosjean and Harrison (1985)
Field campaign	PAN	10–80 ppt min^{-1}	luminol	CL NO_2	Gaffney et al. (1999)
Synthesis	C_3–C_5 alkyl nitrates C_2–C_4 hydroxynitrates C_2–C_4 dinitrates		e^-/luminol	GC-ECD –CL NO_2	Hao et al. (1994)
Laboratory/field campaign	ΣAN, ΣPN	30–90 ppt	–	TD-LIF	Day et al. (2002)
Field campaign	ΣAN, ΣPN	30–90 ppt	–	TD-LIF	Perring et al. (2010)
Field campaign	C_3–C_5 alkyl nitrates	10 ppt	e^- e^-_{th}	GC-ECD GC-NICI-MS	Atlas (1988)
Field campaign	C_2–C_3 Alkyl nitrates PAN, PPN,	10 ppt	e^-	GC-ECD	Fukui and Doskey (1998)
Synthesis; cis-2-butene + OH (NO)	Alkyl nitrates α, β-hydroxynitrates, dinitrates	–	e^-	GC-ECD	Muthuramu et al. (1993)
Peroxyalkyl + NO_2	PAN, PPN, PiBN, MPAN, APAN, PnBN, PBzN	2 ppt	e^-	GC-ECD	Flocke et al. (2005)
Field campaign	C_4–C_{14} alkyl nitrates (C_2–C_8)-alkyl- and phenyl-alkyl- nitrates	1 ppt	e^-	GC-ECD GC-EI-MS	Luxenhofer and Ballschmiter (1994), Luxenhofer et al. (1994)
Field campaign	C_6–C_{13} alkyl nitrates C_3–C_6 dinitrates C_2–C_6 hydroxynitrates		e^-	HPLC / GC-ECD GC-EI-MS	Fischer et al. (2000), Kastler and Ballschmiter (1999)
Field campaign	PAN, PPN, MPAN,	15 ppt (10 min)$^{-1}$	e^- e^-_{th}	GC-ECD GC-NICI-MS	Tanimoto et al. (1999)
Synthesis; alcohols + N_2O_5	C_1–C_8 alkyl nitrates, ketonitrates, hydroxynitrates, dinitrates	–	e^- CH_5^+	GC-ECD GC-NO_y CI-MS	Kames et al. (1993)
NO_3 + α-pinene	Carbonyl hydroxynitrates or PANs	–	H^+ (MeOH)	APCI-MS	Perraud et al. (2010)
Peroxyacetyl + NO_2	PAN, PPN, MPAN	10 ppt (15 s)$^{-1}$	I^-	TD-CIMS	Slusher et al. (2004), Huey (2007)
C_2–C_8 alkenes + OH (O_2, NO)	β-hydroxynitrates	19–50 counts ppb^{-1}	CF_3O^-	ToF CIMS MS-MS CIMS	Teng et al. (2015)
Field campaign	PAN, PPN, MPAN	25 counts ppb^{-1}	O_2^+, H_3O^+, $(H_2O)_2H^+$ H_3O^+	SIFDT[a] PTRMS	Hansel and Wisthaler (2000)
Synthesis	C_1–C_5 alkyl nitrates	15[b] counts ppb^{-1}	H_3O^+	PTRMS	Aoki et al. (2007)
C_3–C_6 Cycloalkanecarbaldehydes	nitroperoxycarbonyl cycloalkyl nitrates	20[b] counts ppb^{-1}	H_3O^+ $H_3O^+(H_2O)_n$	PTRMS	D'Anna et al. (2005)

[a] Selected ion flow drift tube; [b] as specific alkyl ($-R^+$) fragment.
PAN is peroxyacetyl nitrate; PPN is peroxypropionyl nitrate; PiBN is peroxyisobutyryl nitrate; MPAN is peroxymethacryloyl nitrate; APAN is peroxyacryloyl nitrate; PnBN is peroxybutyryl nitrate; PBzN is peroxybenzoyl nitrate.

(Slusher et al., 2004). The CF_3O^- was equally successfully tested as ionizing source in a CIMS approach in order to identify hydroxynitrates formed during the OH oxidation of alkenes in the presence of O_2 and NO (Bates et al., 2014; Teng et al., 2015). The quantification of the nitrates formed was assured by a complementary TD-LIF technique after subsequent GC separation. Other polyfunctional organic nitrates were scarcely detected using this technique.

The proton-transfer-reaction mass spectrometry (PTR-MS) can be positioned as a subset of CI. Its use in atmospheric research has expanded rapidly these last years but few studies have tested this technique for the detection of organic nitrates (Aoki et al., 2007; Hansel and Wisthaler, 2000; Inomata et al., 2013).

The recent study of Müller et al. (2012) considers that the quantification of PAN by PTR-MS is difficult due to

fragmentation. Less promising results are also reported by Aoki et al. (2007) concerning the PTR ionization of C_1–C_5 alkyl nitrates. Considerable fragmentation occurs even at low field density (E/N) ratio (100 Td; E being the electric field strength and N the gas number density; $1\,\mathrm{Td} = 10^{-17}\,\mathrm{V\,cm^2}$), the signal intensities of protonated alkyl nitrates, $(\mathrm{ROH \cdot NO_2})^+$, being in the best case scenario, a few percent of those of the total ion signals. An increase of the E/N ratio increases furthermore the fragmentation, providing common ions such as NO_2^+ and more characteristic ones such as RO^+. Other low-intensity signals corresponding to R^+ or $\mathrm{ROH \cdot H^+}$ ions have been also recorded and could result from reactions of alkyl nitrates with $H_3O^+(H_2O)_n$ clusters.

Hansel and Wisthaler (2000) have measured several PANs (PAN, MPAN and PPN) with PTR-MS and have reported a low detection limit (70 pptv, 15s integration time) and an overall accuracy of 15 %. It is worth noting that the reported analytical sensitivities (15–25 counts $\mathrm{ppb^{-1}}$) have not been calculated for the molecular ion signal but for typical molecular fragments in the case of the alkyl nitrates or signals of speculative subsequent reaction products of the protonated molecular ions for PANs. These results are illustrative of the organic nitrates overall affinity towards fragmentation due to chemical ionization in a low pressure drift tube under high voltage. To our knowledge, polyfunctional organic nitrates have never been detected using this technique.

So, it appears useful to better explore the possibility of detecting organic nitrates in real time with PTR-MS. In the present work, the detection of alkyl and multifunctional organic nitrates (PANs, ketonitrates, hydroxynitrates) by this technique was investigated. For this purpose, different organic nitrates were synthesized and mixtures at the ppb–ppm level were generated in a smog chamber. A commercial PTR-TOF-MS instrument was used but the operating mode as well as the chemical ionization reagent have been modified and optimized for each type of organic nitrate in order to gain sensitivity in the detection and to reduce fragmentation of ions. Mass spectra have been carefully interpreted and detection limits have also been determined.

2 Material and methods

2.1 Instrumentation

A commercially available, high-mass-resolution PTR-TOF-MS instrument (Kore Technology "Series II" High Performance PTR-TOF-MS) was used in the present study. The mass resolution of this instrument is $>5000\,\mathrm{M}/\delta\mathrm{M}$. Mass calibration of the recorded spectra was systematically performed. The procedure allowed us to accurately assign the mass spectra peaks.

The PTR-MS is equipped with the newly designed radio frequency (RF) ion funnel which is used to focus ions in the drift tube and hence to increase the detection sensitivity (Barber et al., 2012). This ion funnel uses a series of electrodes with progressively reducing aperture sizes. In addition to the standard direct current (DC) electrical field, an alternative current (AC) electric field is provided at a radio frequency that creates a strongly repulsive effective potential near the surface of the electrodes, which combined with the reducing aperture sizes serves to focus the ions radially. This system has been shown to increase the sensitivity by 1 or 2 orders of magnitude (Barber et al., 2012). It is worth noting that operating in the RF mode modifies the dynamic range over which the drift tube is operated and the contribution of the radio frequency to the global effective E/N ratio remains difficult to estimate (Barber et al., 2012).

The PTR-MS sampling line was designed in order to assure the highest transfer efficiency of the compounds. This line is made of a 1.5 m long Silcosteel® coated stainless steel tubing (2.1 mm inner diameter), which has been shown to be appropriated for the transfer of low-level polar organic compounds (Smith, 2003). This line was heated at 40 °C as a compromise between the thermolability of the organic nitrates and the condensation processes. With a sampling flow rate of $\sim 3\,\mathrm{cm^3\,s^{-1}}$, the residence time in the line has been estimated to be lower than 2 s. The PTR-MS inlet system is equally temperature controlled and made with Silcosteel® coated stainless steel tubing. Running the system at ambient temperature-induced PTRMS signal instability, while subsequent heating of the sampling line revealed desorption processes (peaks of analytes following the heating steps).

2.2 Experimental strategy

In PTR-MS, proton transfer reactions with hydronium ions (H_3O^+) are typically used to ionize compounds having a proton affinity (PA) higher than that of water (691 $\mathrm{kJ\,mol^{-1}}$; Hunter and Lias, 1998):

$$\mathrm{H_3O^+ + R \rightarrow RH^+ + H_2O}. \quad \text{(R1)}$$

In this case, the proton transfer reaction is exothermic and proceeds at a reaction rate close to the collision rate ($10^{-9}\,\mathrm{cm^3\,molecule^{-1}\,s^{-1}}$; Flocke et al., 1991). In order to avoid a massive fragmentation of the analyte and consequently a decrease of the intensity and the specificity of the analytical signal, the energy transferred during the reaction should be lower than the bond energies of the compound of interest.

Only few available data can be found concerning the PA of organic nitrates, which were calculated using ab initio quantum mechanical methods exclusively. The PA of organic nitrates has been estimated to be $740\,\mathrm{kJ\,mol^{-1}}$ for methyl nitrate (Lee and Rice, 1992), $753\,\mathrm{kJ\,mol^{-1}}$ for ethyl nitrate (Kriemler and Buttrill, 1970), $748\,\mathrm{kJ\,mol^{-1}}$ for methyl peroxynitrate (Ravelo and Francisco, 2007) and 759–$773\,\mathrm{kJ\,mol^{-1}}$ for peroxyacetyl nitrate (Tureček, 2000). These studies show that the PA of organic nitrates is higher than

that of water, so that proton transfer reaction may occur. Furthermore, the functionalized nitrates concerned by the current study are equally expected to easily protonate as it was shown that the presence of an additional oxygen atom in the molecule enhances the overall PA (Ravelo and Francisco, 2007).

It is well known that other chemical processes can also occur in the PTR reactor (Blake et al., 2009; de Gouw and Warneke, 2007). The H_3O^+ and R^+ can cluster with water molecules in the sampled air. The water cluster ions formation in the PTR cell is generally considered as problematic since their presence complicates the mass spectra treatment. Typically, their formation is limited by high kinetic energy of the ions into the drift tube at E/N ratios superior to 100 Td. However, the proton transfer reaction of $H_3O^+(H_2O)_n$ clusters is more selective than the H_3O^+ due to a higher PA (808 kJ mol^{-1}; Goebbert and Wentold, 2004). This property may be valuable in our case as it allows a softer ionization of analytes. Recently Jacobs et al. (2014) have used $H_3O^+(H_2O)_n$ ions (distribution centered around $n = 4$) in PTR-CIMS technique with the objective of monitoring isoprene-derived hydroxynitrates and their oxidation products. In order to evaluate the efficiency of the protonation mode by $H_3O^+(H_2O)_n$ for the detection of other organic nitrates, a wide range of E/N ratios will be tested.

The NO^+ chemical ionization has also been tested for the detection of organic nitrates during our experiments. It has been shown to be a complementary, sensitive and reliable method for the detection of some organic compounds such as ketones, aldehydes and alkenes by CIMS and SIFT-MS techniques (Knighton et al., 2009; Mochalski et al., 2014; Perraud et al., 2010; Wang et al., 2004). NO^+ ions are produced from the ionization of dry air within the hollow cathode discharge ion source. This process produces large amounts of NO^+ with only minor amounts of NO_2^+, O_2^+ and $H_3O^+(H_2O)_n$ impurities (Knighton et al., 2009). The intensities of O_2^+ and $H_3O^+(H_2O)_n$ are quite low – less than 1 % of the primary NO^+ signal. In addition, it has been shown that the intensity of the NO_2^+ impurity is controllable and dependant on how the hollow cathode ion source is operated (Knighton et al., 2009). The ion source extraction voltage and the hollow cathode discharge current are the two most important parameters.

Previous studies interrelated the PA of water to the NO^+ chemical ionization binding energies (BEs), creating an absolute NO^+ affinity scale (Cacace et al., 1997). The study used the H_2O–NO^+ BE as a reference anchor between the two conjugated parameters and concerned various classes of ligands (alkyl halides, alkyl nitrates, alcohols, nitro-alkanes, nitriles, aldehydes, ketones, aromatic and heterocyclic compounds). With the exception of the aromatic compounds, for which the $NO^+\sigma$-type complex structures are replaced by the π complexes, the overall data exhibit a highly correlated linear dependence ($BE_{NO}+ = 0.367\,PA - 174.5$ kJ mol^{-1}). When compared with protonation energies, the BEs characterizing the NO^+ chemical ionization are significantly lower (Cacace et al., 1997).

This characteristic offers the opportunity to generate soft ionizations with little fragmentation of the product ions, which is of high interest for the present study. Reactions which may occur are

$$NO^+ + R \rightarrow R^+ + NO, \quad \text{(R2a)}$$

$$NO^+ + R \rightarrow R \cdot NO^+, \quad \text{(R2b)}$$

$$NO^+ + RX \rightarrow R^+ + XNO \quad (X = \text{–H, –OH, –CH}_3\text{, –OR}). \quad \text{(R2c)}$$

As a function of the chemical affinity, NO^+ chemical ionization may follow several pathways. The charge transfer Reaction (2a) seems to be the most common process for compounds having ionization energies slightly lower or close to that of NO (IE = 9.26 eV) (e.g., isoprene (Karl et al., 2012) butadiene, benzene (Knighton et al., 2009), monoterpenes, terpenoids (Amadei and Ross, 2011; Rimetz-Planchon et al., 2011) and phenols (Wang et al., 2004)). This hypothesis is confirmed by Smith et al. (2003), who reported for a series of ketones (C_3–C_{11}) that the yields of parent radical cation increase as the IE decrease.

The adduct formation pathway (Reaction 2b) has been previously reported for the detection of C_3–C_4 alkanes, alkenes and terpenes (Diskin et al., 2002; Španěl and Smith, 1998), ketones (Smith et al., 2003; Wang et al., 2004) and flavoring esters (Iachetta et al., 2010) by selected ion flow tube mass spectrometry. The speculated mechanism which has been proposed to explain the formation of the adduct involves the formation of an excited intermediate complex $(R \cdot NO^+)^*$, which is then stabilized by collision with the carrier gas (Smith et al., 2003). Evidently the process is enhanced at upper PTR reactor pressure involving higher collision rates.

A third mechanism, similar to the protonation, involves the hydride, hydroxide, methyl or alkoxy abstraction (Reaction 2c), as reported for aldehydes, ethers, alcohols (Smith and Španěl, 2005), terpenoids (Amadei and Ross, 2011) or several unsaturated alcohols (Karl et al., 2012; Schoon et al., 2007; Wang et al., 2004).

The O_2^+ ionization can generate artifacts, particularly when the PTR-MS is operated in dry air mode, as it proceeds via a dissociative charge transfer reaction, producing parent cations M^+ as well as fragment ions. As a consequence, this process is of little interest for chemical ionization of large molecules.

To summarize, several parameters will be tested in order to establish the optimal conditions for the detection of each class of organic nitrates.

A carefully thought-out procedure was performed in order to establish the optimal measurement conditions for each class of organic nitrates:

– First, the instrument has been used in a dual mode, employing alternatively H_3O^+ and NO^+ as a reagent ion

by shifting the glow discharge (GD) source gas from water vapor to dry air. Dry air was supplied to the hollow cathode ion source using the alternative GD ionization line. A third operation mode which consists of suppressing the GD source gas once the plasma is established has also been tested. This last operational mode implies hence the retro-diffusion of the sampling line dry air into the GD cavity and will be further referred to as the retro-diffusion mode (RDiff).

- The ion intensity and distribution are sensitive to the extraction voltage used to inject the reagent ions into the drift tube and to the hollow cathode discharge current. The PTR-MS instrument was thus operated in a wide range of E/N (electric field to number density of the gas) ratios (30–180 Td), hence shifting the distribution between the different ionizing analytes in the protonation mode (H_3O^+ / $H_3O^+(H_2O)_n$) or into the dry air mode (NO^+ / NO_2^+).

- The sampling line and the inlet system along with the drift tube was slightly heated (40 °C) and the reactor pressure ranged from 0.7 to 1.6 mbar. The sampling flow rate (2.9 to 3.5 $cm^3\ s^{-1}$) affects through the mass of the sampled analyte or through the third body collision processes the instrument response. An enhanced influence of this parameter may be noticed while operating in the RF mode.

- The influence of radio frequency ion funnel mode on the detection of the various organic nitrates has been tested by performing experiments with the RF mode on and off.

Ideally, little or no fragmentation occurs in the case of a soft ionization process. The large differences in ionization energy of the colliding species enhance the fragmentation of the organic molecule. Therefore the ionizing gas species should correspond, especially for labile molecules, to the analyte of interest in order to achieve the high yield ionizations with low excess energy.

In addition, the soft ionization processes demand the usage of uncommon settings of the PTR-MS device. The various effects of the altered PTR-MS tuning are termed in detail elsewhere (Hewitt et al., 2003; Knighton et al., 2009). Supplementary information relating the ion source discharge current and the extraction voltage influence is discussed in the Sect. 3.

All reported signal intensities took systematically into account the background values, representing in most of the cases negligible low values of a few counts per minute. Background measurements are achieved before every single experiment by sampling the dry synthetic air of the reaction chamber.

2.3 Normalizing analytical signal for H_3O^+ and NO^+ ionization

In this study, calibrated response factors of PTR-MS are determined for several types of organic nitrates in both H_3O^+ and NO^+ ionization modes. For that purpose, known amounts of organic nitrates are introduced in LISA simulation chamber (see following section). To quantify the PTR-TOF-MS response factors (S; ncpm $ppbv^{-1}$), the ion signal (I_{R^+}; ncpm) is divided by the known concentration of organic nitrate ($ppbv^{-1}$), as measured by the FTIR in situ technique. Corrections of the product ion signal (I_{R^+}) due to changes of the operational conditions have to be taken into account, as shown by previous studies (Knighton et al., 2009):

$$I_{R^+} = \left(\frac{i_{R^+}}{f_{IA^+}}\right)\left(\frac{P_0}{P}\right)^2\left(\frac{T}{T_0}\right)^2. \quad (1)$$

The intensity of the product ion raw signal (i_{R^+}) expressed in counts per minute is adjusted to the variabilities of the ionizing analyte (i_{IA^+}) normalized to its averaged values ($\langle i_{IA^+}\rangle$), ($f_{IA^+} = i_{IA^+}/\langle i_{IA^+}\rangle$; $IA^+ = H_3O^+$ or NO^+) as it has been shown that both signals (i_{R^+} and i_{IA^+}) are related. The drift tube temperature (T) and pressure (P) are also included in this expression to account for the small changes in the reaction time and gas number density that can occur during measurements. In our experiments, the temperature was very stable (±1 K) but the PTR pressure was affected by the pressure in the simulation chamber, which usually slowly decreases because of the sampling from the constant volume of the rigid chamber.

Due to the high abundance of the ionizing species, the direct measurement of H_3O^+ and NO^+ reagents was not possible as the ion counting signals (m/z 19 and 30) were regularly saturated. The natural isotopic abundance properties of ^{17}O (0.038 % of O), ^{18}O (0.200 % of O) and ^{15}N (0.368 % of N) are used to overcome this drawback and evaluate the primary H_3O^+ and NO^+ ion intensity using the m/z 21 ($H_3^{18}O$) and 31 respectively ($\Sigma^{15}NO^+$ and $N^{17}O^+$) (De Laeter et al., 2003). The $I_{H_3O^+} = I_{m/z21} \times 500$ and $I_{NO^+} = I_{m/z31} \times 247$ formulas were applied as a result of isotopic abundance probability calculations.

2.4 LISA atmospheric simulation chamber

Gaseous mixtures of organic nitrates at the ppb–ppm level were generated in the simulation chamber at LISA. This chamber comprises a Pyrex reactor of 977 L equipped with a multiple reflection optical system interfaced to a FTIR spectrometer (Vertex 80 from Bruker). Details of this smog chamber are given elsewhere (Doussin et al., 2003).

All experiments were conducted in the dark at 298 ± 2 K and atmospheric pressure. Mixtures of organic nitrates were generated in synthetic air (N_2 80 % + O_2 20 %) by introducing a known amount of the organic nitrate into the chamber and cross-monitored by long-path in situ FTIR and PTR-MS

techniques. Concentrations of organic nitrates were checked from their infrared spectral absorption bands. Integrated band intensities (IBIs; expressed in cm molecule^{-1} and calculated in decimal logarithm) and the spectral integration areas used to quantify PAN-like compounds and other nitrates are 9.50×10^{-18} for PANs (765–812 cm^{-1}), 8.30×10^{-18} for alkyl nitrates (820–900 cm^{-1}), 1.17×10^{-17} for hydroxynitrates (816–882 cm^{-1}) and 1.08×10^{-17} for ketonitrates (820–870 cm^{-1}). The IBIs are given by Allen et al. (2005) and Spittler (2001) for the PANs and the hydroxynitrates, respectively, whereas in the current study for the alkyl nitrates and ketonitrates the IBIs were calculated from repetitive injections of known amounts of analyte. It is worth noting the weak disparity of cross sections concerning the characteristic $-ONO_2$ absorption band. Reference gas-phase FTIR absorption spectra of the synthesized organic nitrates (KnC3, KnC5, 1OH3C3) are plotted in Fig. S1 in the Supplement and compared with the recorded spectra of a commercially available alkyl nitrate (AlkC3).

Before and after every single experiment, a cleaning procedure was applied in order to avoid memory effects from an experiment to the next one. It consists of vacuum clean-up down to 10^{-2} mbar for at least 10 h and UV irradiation (340 and 360 nm fluorescent tubes) in order to heat the reactor and improve desorption of semi- and low-volatile compounds from the walls.

2.5 Chemicals and gases

The simulation chamber was filled with dry synthetic air generated with N_2 (from liquid nitrogen evaporation, > 99.995 % pure, < 5 ppm H_2O; Linde Gas) and O_2 (quality N45, > 99.995 % pure, < 5 ppm H_2O; Air Liquide). Supplementary cylinder air was used for the dry air glow discharge generation in PTR-MS (AlphaGaz™ 2; $H_2O < 0.5$ ppm; $C_nH_m < 50$ ppb; $CO_2 < 0.1$ ppm; $CO < 0.1$ ppm; $NO_x < 10$ ppb).

The alkyl nitrates considered in the present study (n-propyl nitrate – 97 % Janssen Chimica; AlkC3 and isobutyl nitrate – 96 % Sigma Aldrich; AlkiC4) were used as commercially available, without further purification.

Ketonitrates were synthesized using Kames' method, (Kames et al., 1993): a liquid/gas-phase reaction in which the corresponding hydroxy ketone is reacted with NO_3 radicals released from the dissociation of N_2O_5, at ice bath temperature, under dry condition. The carbonyl nitrates and nitric acid were separated by multiple vacuum headspace procedure. The carbonyl nitrates' structure and purity were verified by FTIR. In addition, it was checked by GC-MS that the organic reactant used for the synthesis, here the hydroxy ketone, was fully consumed, preventing any interference in IR and mass spectra. The presence of HNO_3 is regularly noticed since it is injected as byproduct of the carbonyl nitrates synthesis. 1-hydroxy-2-propanone (95 % Alfa Aesar) and 3-hydroxy-3-methyl-2-butanone (97 % Sigma Aldrich) were used for the synthesis of 1-nitroxy-2-propanone and 3-nitroxy-2-propanone respectively.

The hydroxynitrate was synthesized starting from the commercially available 3-bromo-1-propanol (97 % Sigma Aldrich). Its conversion to the analog iodide was performed by a Finkelstein reaction with sodium iodide (Baughman et al., 2004) and the subsequent mild conversion with $AgNO_3$ (Castedo et al., 1992) leading to the formation of 1-hydroxy-3-nitroxy-propane (1OH3C3). The total consumption of the bromo-alcohol was checked by GC-MS.

The PAN-type compounds were generated in the simulation chamber from the gas-phase oxidation of corresponding aldehydes by NO_3 radicals (Hanst, 1971). In our experiments, PAN was formed from the oxidation of acetaldehyde (> 99.5 % Sigma Aldrich). This reaction has been shown to produce mainly PAN with a yield close to 70 % (Doussin et al., 2003).

The presence of impurities as synthesis byproducts may add supplementary signals in the PTRMS mass spectra. These signals are, however, systematically at lower masses than those in the main ionization processes of the organic nitrates and therefore will not interfere in the main frame of the discussion.

3 Results and discussion

3.1 Influence of the operating conditions on the ionizing analytes signals

As already termed, intensities and mixing ratios of the ionizing species are dependent on the E/N ratio. For a standard drift tube, E/N is a well-defined quantity but, when the instrument is run in RF mode, the influence of the additional AC electric field on the E/N ratio has to be taken into account and this is not obvious. Barber et al. (2012) have attempted to empirically estimate an effective E/N by running the instrument with the RF mode on and off and by seeking operating conditions for the RF on mode that match the performance obtained when the RF mode is off. The criterion used to estimate the performance is the ratio $[H_3O^+] / [H_3O^+(H_2O)]$. During our experiments, the additional AC electric field was fixed. Thus, variations of E/N ratio result only from variations of the DC component of the drift tube.

Typically recorded distributions over a relevant range of E/N are illustrated in Fig. 1 for both ionization modes, with and without the above described RF mode. When the RF mode is not employed, the water cluster ion distribution obtained in this study (Fig. 1) is in reasonable agreement with those calculated and measured by de Gouw and Warneke (2007), asserting that (i) the $H_3O^+(H_2O)_2$ cluster is abundant for E/N ratios < 60 Td, (ii) the $H_3O^+(H_2O)$ signal is maximum around 80 Td and (iii) the H_3O^+ signal is predominant for values larger than 100 Td. In the RF mode,

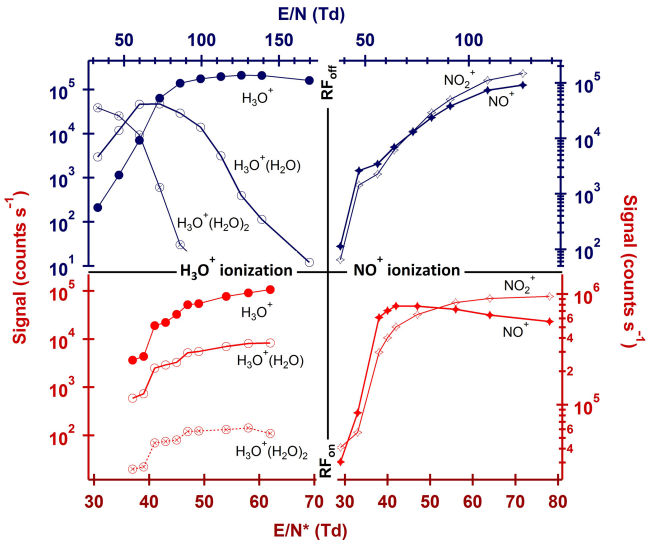

Figure 1. Typical ionizing species distribution as a function of the E/N ratio, in the two ionization modes with RF mode on and off. When the RF mode is on, E/N^* ratios were calculated taking into account only the contribution of the DC electric field while the additional input of the AC electric field remains difficult to estimate.

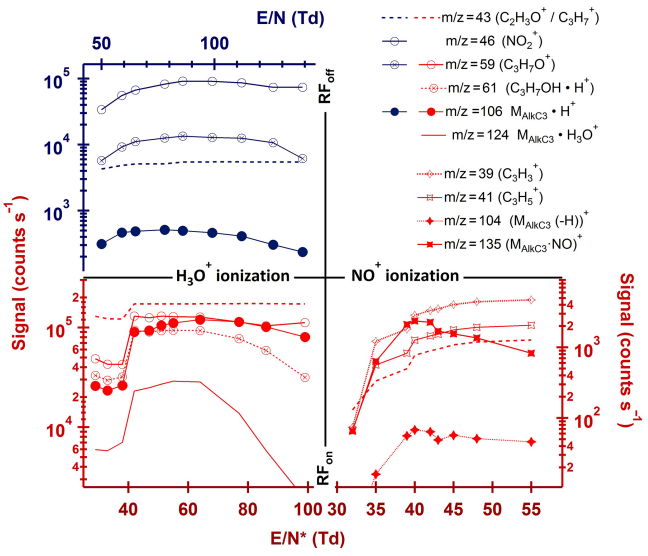

Figure 2. The E/N ratio influence over the AlkC3 identification for several representative signals in both ionization modes (H_3O^+, left; NO^+, right) as recorded in absence (up)/presence (down) of a RF funnel. The common signal at $m/z = 43$ is equally plotted as a fragmentation mark (right axis).

it has been observed that the signal of H_3O^+ ion is much higher than those of clusters for the entire range of E/N ratios. The $H_3O^+(H_2O)$ is 1 order of magnitude lower than the H_3O^+ and 1 order of magnitude more abundant than the $H_3O^+(H_2O)_2$. As the distributions of ions obtained with and without RF mode are quite different, it was not possible to estimate an effective E/N as proposed by Barber et al. (2012). So E/N ratios have been calculated without taking into account the RF contribution. In the case the RF mode is on, E/N ratios are indicated with * (E/N^*).

The NO^+ ionization mode has been found more promising in the RF mode, since the abundance of the ionizing species is largely superior. Furthermore, the NO^+/NO_2^+ ratio exhibits the highest values around 40 Td in the RF mode, increasing the probability to form the analyte-NO^+ adduct. Therefore, all further results presented in the current work in the NO^+ mode have been recorded with the RF mode and reported E/N^* was calculated without taking into account the AC radio frequency contribution.

3.2 Alkyl-nitrates

3.2.1 H_3O^+ ionization mode

A series of tests has been conducted in order to seek the optimum operating conditions for the measurement of alkyl nitrates with H_3O^+ ionization mode. In particular, the E/N ratio was spanned in the 50–140 Td range. The intensity of the main signals obtained for n-propyl nitrate (AlkC3) with the RF mode off has been plotted as a function of E/N in Fig. 2. The recorded mass spectra of AlkC3 are characterized by a high degree of fragmentation, even for the lowest E/N (50 Td). The AlkC3 mass spectra recorded at the lowest extent of fragmentation of the protonated molecular ion is illustrated by Fig. 3a. The same result has been observed for AlkiC4 as depicted by the Fig. S2 in the Supplement. Consequently, the sensitivity of the molecular ions formed is low (see Table 2). The protonated alkyl nitrates are expected to adopt the ion-dipole complex conformation ($ROH \cdot NO_2^+$; R1a) and not a covalently bound $RONO_2H^+$ one (Cacace and de Petris, 2000).

$$H_3O^+ + RONO_2 \rightarrow ROH \cdot NO_2^+ + H_2O \quad \text{(R1a)}$$

The bound energy of these complexes was calculated by ab initio methods to be around 82 kJ mol^{-1} in the case of methyl nitrate (Lee and Rice, 1992).

The only other study (Aoki et al., 2007) describing a tentative of alkyl nitrate detection with PTR-MS used E/N ratio spanning between 96 and 147 Td. The low BE characterizing the formed complex enables its decomposition in ROH and NO_2^+ by collision-induced dissociations. The recorded signals of NO_2^+ (m/z 46) and RO^+ (m/z 59 for AlkC3 and 73 for AlkiC4) are probably formed by the mechanisms:

$$ROH \cdot NO_2^+ \rightarrow ROH + NO_2^+, \quad \text{(R2)}$$

$$ROH \cdot NO_2^+ \rightarrow RO^+ + HONO. \quad \text{(R3)}$$

This statement is supported by the decrease of the protonated signal in conjunction with the increase of the NO_2^+ with increasing E/N.

The presence of the m/z 43 (AlkC3) and 57 (AlkiC4) signal was clearly identified as the alkyl fragment (R^+) of ni-

Table 2. Organic nitrates normalized sensitivity as a function of the ionization mode.

Compound	MW (g mol^{-1})	H_3O^+ ionization			NO^+ ionization		
		Signal (m/z)	Sensitivity (ncpm) ppbv^{-1}	E/N (Td)	Signal (m/z)	Sensitivity (ncpm) ppbv^{-1}	E/N (Td)
AlkC3	105	43	35	70	*104*	1.1	34*
propyl nitrate		59	18.8		*135*	48.8	
		106	2				
AlkiC4	119	57	43.4	70	*118*	8.3	34*
isobutyl nitrate		73	23		149	78.9	
		120	2				
KnC3	119	75	45.4–88.4	73–75	149	320–331	45*
nitroxyacetone		120	119–144	73–75			
		137	127	48*			
KnC5	147	103	38.3	74	177	249–265	39*
3-nitroxy-3-methyl-		148	8	74			
2-butanone		165	538	48*			
PAN	121	122	7.7	90	151	weak	
1OH3C3	121	104	0.2	62	120	22.8	34*
1-hydroxy-3-nitroxy-		120	0.2		151	268	
propane		122	2		167	10.2	
		139	52.6				
		140	38				

* Without taking into account the RF contribution.

trate by the means of high-resolution mass spectrometer allowing us to differentiate between oxygen containing analytes and alkyl fragments.

At higher abundances of the water clusters, expected to occur in our study due to the usage of low E/N ratios, the R5 mechanism is considered more likely, as proposed by Aoki et al. (2007). The formation of R–OH $\cdot$ H$^+$ ion can also be explained by Reaction (R6) as proposed by Spanel and Smith (1997). This ion is then expected to form the alkyl fragment (R$^+$) by Reaction (R7):

$$RONO_2 + H_3O^+(H_2O)_n \rightarrow R\text{-}OH \cdot H^+ + HNO_3 + nH_2O, \quad (R4)$$

$$RONO_2 \cdot H^+ + H_3O^+ \rightarrow R\text{-}OH \cdot H^+ + HNO_3, \quad (R5)$$

$$R\text{-}OH \cdot H^+ \rightarrow R^+ + H_2O. \quad (R6)$$

A third option is to consider the direct formation of the alkyl fragment from the collision-induced dissociation of the protonated alkyl nitrates formed in Reaction (R1a) into R$^+$ and HNO_3. Further collisions of the alkyl fragment ($R^+ = C_3H_7^+$) might generate the loss of two hydrogens and explain the weak signals at m/z 41 in the case of AlkC3.

$$C_3H_7^+ \rightarrow C_3H_5^+ + H_2 \quad (R7)$$

It should be noticed that the analog process for the m/z 55 in the case of AlkiC4 cannot be observed since it falls near a relatively abundant water cluster signal.

Results obtained with the RF mode are equally shown in Fig. 2 for the AlkC3 for comparison. The ionization pattern of the analyte is slightly different from the one obtained without RF mode and enables, adjacent to the formation of the protonated alkyl nitrate, the identification of other specific signals like the adduct AlkC3 $\cdot$ H_3O^+ formation. Characterized by a high degree of fragmentation, the spectra contain the protonated ion-dipole complex ROH $\cdot$ NO_2^+ at $m/z = 106$ (Reaction R1a) with the highest sensitivity above 60 Td. The E/N ratio is calculated without taking into account the RF contribution. The m/z 124 signal can be assigned to the AlkC3–H_3O^+ adduct formation. An analog process is described in the literature for long alkanes (>C6) providing M $\cdot$ H_3O^+ signals (Španěl and Smith, 1998), in contrast with the alkenes which are readily protonated due to their higher PA.

The alkyl (R$^+$) intermediary parent ion, described in R5 and R6 (R–OH $\cdot$ H$^+$), is equally recorded, corresponding in the case of AlkC3 to the m/z 61 signal. The increase of the E/N ratio over 60 Td contributes to a higher degree of decay of this intermediate ion in the particular conditions of the RF mode. The RO$^+$ ion at m/z 59 is equally present in the case of AlkC3, confirming the existence of the Reaction (R4) mechanism leading to HONO formation.

To summarize, the use of H_3O^+ ionization is not really suitable for the detection of alkyl nitrates as it leads to high

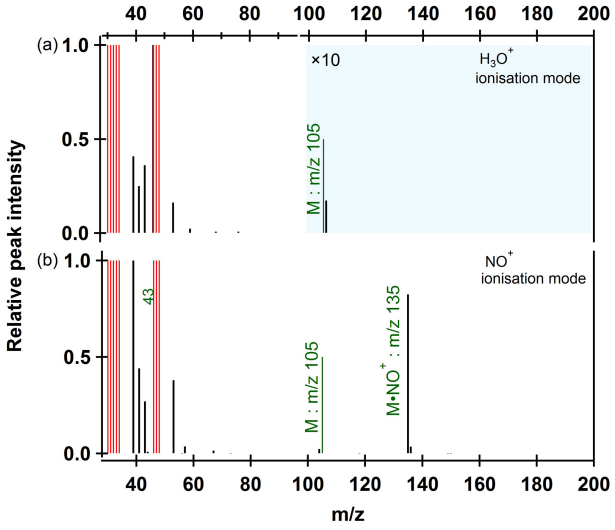

Figure 3. Recorded mass spectrum of AlkC3 (black bars) at the lowest extent of fragmentation of the molecular ion at $m/z = 106$ ($E/N = 78$ Td) in the H_3O^+ ionization mode in absence of the RF **(a)** and in the NO^+ ionization mode at $m/z = 135$ in presence of the RF ($E/N^* = 34$ Td) **(b)**. The thin green line represents the expected molecular ion of the analyte. The intense signals depicted by the red thin bars represent the ionizing and matrix analytes at $m/z = 30$ (NO^+) and 46 (NO_2^+) and their isotopic abundance signals at $m/z = 31$ and 47, 48 respectively. The signals corresponding to the water clusters ($H_3O^+(H_2O)_n$ at m/z 37 and 55 are systematically erased for simplification.

fragmentation, even at low E/N ratios, hence generating intense signals of common organic analytes, unsuitable for a reliable identification of these compounds. In addition, if considering the more characteristic signals of the protonated ion-dipole complex ROH· NO_2^+, the H_3O^+ ionization mode exhibits a poor detection limit: 5 ppb min^{-1} for both AlkC3 (m/z 106) and AlkiC4 (m/z 120). This detection limit was estimated for a mean signal to noise ratio of 3 at the chosen m/z.

In Table 2, the characteristic signals of each organic nitrate studied here as well as their detection limits are listed.

3.2.2 NO^+ ionization mode

The performances of the NO^+ ionization were also evaluated. The most promising results, enabling the identification of characteristic signals of the studied alkyl nitrates, were obtained in the RF mode. The scan of a large range of E/N^* ratios confirmed that the highest sensitivity towards NO^+-induced ionization and identification is obtained around 40 Td as illustrated in Fig. 2 for the AlkC3 case. As mentioned previously, the calculated E/N ratio does not take into account the RF contribution to the ion funnel field.

The recorded mass spectra of the analyte of interest in terms of relative peak intensities as a function of the m/z are represented by the thick black lines in Fig. 3b. It should be kept in mind that the NO^+ and NO_2^+ signals illustrated above are the sum of the corresponding nitrate fragments as well as the ions formed into the dry air plasma GD. The presence of O_2^+ ($m/z = 32$) and its interfering isotopic abundance signals at $m/z = 33$ and 34 has been observed and could result in interfering signals.

For both alkyl nitrates, the adduct formation (Reaction R2b) appears to be the main ionization mechanism under these given conditions, leading to intense peaks at $m/z = 135$ (10 5+ 30) and $m/z = 149$ (119 + 30) for AlkC3 and AlkiC4 respectively (see Figs. 3b and S2b). The hydride abstraction $(R(-H))^+$ was also detected as a minor pathway (Reaction 2c) at $m/z = 104$ and $m/z = 118$ for AlkC3 and AlkiC4 respectively. Despite a weak intensity, this signal can be used as an interrelated identification signal for alkyl nitrates. The fraction of the abstraction channel is at no time higher than 10 % of the intensity of the adduct formation channel.

An intense peak corresponding to the alkyl fragment (R^+) was observed in spectra at m/z 43 (AlkC3) and 57 (AlkiC4). The alkyl fragment signal is followed by a downward series of signals at m/z 41 and 39 in the case of AlkC3 and at m/z 55 and 53 for the AlkiC4. Considering the collisions of the alkyl fragment mechanism generating the loss of two hydrogens (Reaction R8), as proposed by Aoki et al. (2007) for the protonation mode, could explain the recorded signals.

In conclusion, the NO^+ ionization mode appears to be more suitable for the detection of alkyl nitrates than the H_3O^+ ionization mode as it produces two characteristic signals, corresponding to the adduct formation ($M \cdot NO^+$) and the hydride abstraction ($M(-H)^+$). The detection limit for the $M \cdot NO^+$ signal was estimated to be 205 ppt min^{-1} for AlkC3 (m/z 135) and 126 ppt min^{-1} in the case of AlkiC4 (m/z 149) (see Table 2). Although superior to the protonation mode, the NO^+ ionization exhibits a poor sensitivity. For measurements in real atmosphere, where alkyl nitrates mixing ratios are usually in the ppt level, accumulations for several hours will be necessary.

3.3 Hydroxynitrates

3.3.1 The H_3O^+ ionization

As for alkyl nitrates, the measurement of hydroxynitrates by PTR-MS has been tested with H_3O^+ ionization mode, with and without RF mode. For this purpose, 1-hydroxy-3-nitroxy-propane (1OH3C3) was synthesized and used as a reference. In the classical mode (RF off), the main signals which have been attributed to 1OH3C3 are m/z 43 ($C_2H_3O^+$), m/z 104 ($M_{1OH3C3}(\text{-OH})^+$), m/z 122 ($M_{1OH3C3} \cdot H^+$) and m/z 139 ($M_{1OH3C3} \cdot H_2O)^+$). Intensities of these signals have been plotted as a function of E/N in Fig. 4. As expected, the intensity of the signal m/z 43 increases with high E/N ratio while protonation and water adduct formation are favored by low E/N. A possible explanation for the formation of the ion $M_{1OH3C3}(\text{-OH})^+$ is a

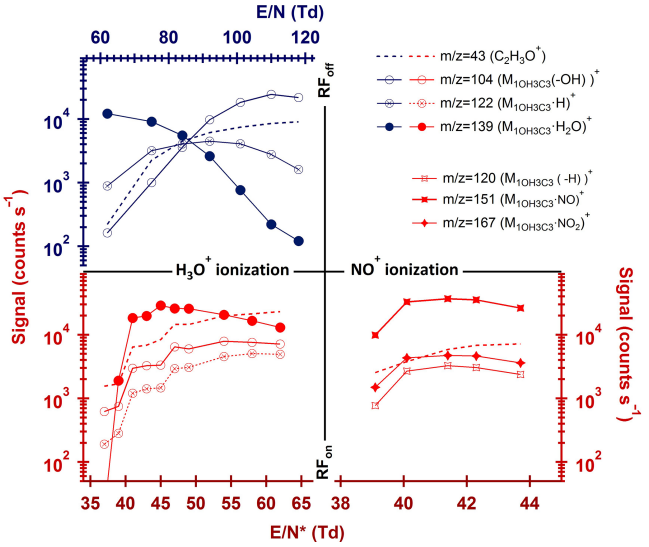

Figure 4. The E/N ratio influence over the 1OH3C3 identification for several representative signals in both ionization modes (H_3O^+, left; NO^+, right) as recorded in absence (up) / presence (down) of a RF funnel. The common signal at $m/z = 43$ is equally plotted as a fragmentation mark (right axis).

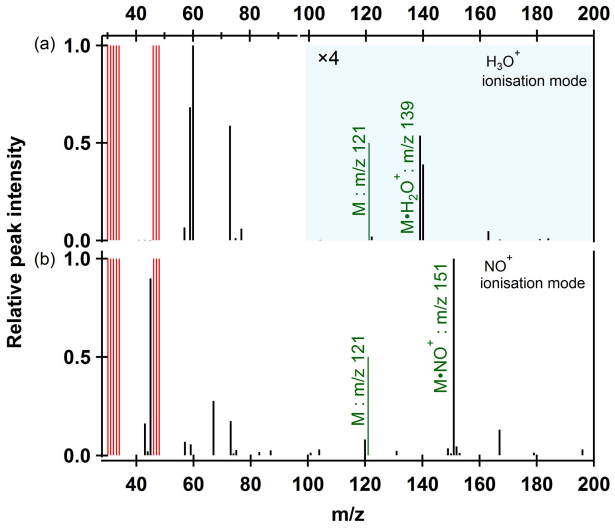

Figure 5. Recorded mass spectrum of 1OH3C3 (black bars) at the lowest extent of fragmentation of the molecular ion ($E/N = 62$ Td) in the H_3O^+ ionization mode in absence of the RF device **(a)** and in the NO^+ ionization mode in presence of the RF ($E/N^* = 41$ Td) **(b)**. The thin green line represents the expected molecular ion of the analyte. The intense signals depicted by the red thin bars represent the ionizing and matrix analytes at $m/z = 30$ (NO^+) and 46 (NO_2^+) and their isotopic abundance signals at $m/z = 31$ and 47, 48 respectively. The signals corresponding to the water clusters $(H_3O^+(H_2O)_n$ at m/z 37 and 55 are systematically erased for simplification.

loss of H_2O after protonation of the hydroxyl nitrate, as suggested by several studies for alcohols (Schoon et al., 2007; Smith et al., 2012; Tuazon et al., 1999).

When the RF mode is on, the same signals (43, 104, 122, 139) were observed but with different relative abundance. The influence of E/N on the intensity of these signals has been equally plotted in Fig. 4. Above 40 Td, the signal characterizing the water adduct formation ($m/z = 139$) is more abundant in the RF mode with a maximum around 45Td.

The water clusters are probably abundant in the PTR reactor due to the low E/N ratios and dissociate only into the RF region after the ionization occurs.

The mass spectrum illustrated by Fig. 5a was recorded in absence of the RF funnel and is dominated by fragments like m/z 59, 60, 73, while the specific signal of the protonated molecule m/z 122 is present close to the noise limit.

The above described water adduct formation ($m/z = 139$) is competed by a H_3O^+ adduct ($m/z = 140$), equally present into the spectra. The ionization is probably induced by the expected high levels of water cluster, following an analogous process with the one described in R5. This involves the release of HNO_3 and arise the signal at m/z 77 (C_3H_6OH)-$OH \cdot H^+$ and subsequently at m/z 59 with the loss of supplementary water (Reaction R7). Further collisions of the above-mentioned ions may well explain the signals at m/z 75 and 57, generated by the loss of two hydrogens (Reaction R8).

In RF mode, the mass spectrum obtained for 1OH3C3 at $E/N^* = 45$ Td (corresponding to the operational condition for which the signal at m/z 139 is the most intense) was illustrated in Figs. 5 and S3. It is worth noticing that all the other competitive ionization processes are strongly diminished in comparison to the spectrum obtained in classical mode. Only the specific signal at $m/z = 104$ exhibits a stronger signature compared to the case above. The fragmentation pattern is strongly diminished in this case.

To conclude, it has been observed that protonation of the hydroxynitrate is a minor process in comparison to fragmentation and to adduct formation. The use of the RF mode significantly reduces the fragmentation for the benefit of the $M \cdot H_2O^+$ adduct formation. The lowest DL (80 ppb min^{-1}) was obtained at 45 Td* in the RF mode for the signal corresponding to the water adduct formation at m/z 139. The same signal in absence of the RF effect is at least twice weaker in terms of sensitivity. Sensitivities of other specific signals are equally proposed for comparison in Table 2.

3.3.2 The NO^+ ionization

The detection of hydroxynitrates in NO^+ ionization mode has been evaluated for the first time by varying the E/N ratio (39–44 Td) and by studying the influence of the RF mode. As stated before the highest sensitivity towards the NO^+ adduct formation is obtained in the RF mode, most likely due to the higher abundance of the ionizing species, as already seen in Fig. 1.

Results obtained with RF mode are shown in Fig. 4. The main signals that have been observed are 151 and 167, which have been attributed to $M \cdot NO^+$ and $M \cdot NO_2^+$ adduct formation, and 43 ($C_2H_3O^+$), which is characteristic of fragmentation. Although weak, the hydride abstraction (Reaction R2c) leading to a signal at m/z 120 has also been observed in the recorded spectra. This process has already been observed in previous studies for various saturated and unsaturated alcohols (C_{1-10}) and phenol (Karl et al., 2012; Schoon et al., 2007; Spanel and Smith, 1997) using SIFT and PTR-MS techniques. The hydride ion transfer of these compounds generates the corresponding carboxy ion (and HNO), while the hydroxide ion transfer gives the corresponding hydrocarbon ion (and HNO_2). Assuming the corresponding ionization of hydroxynitrate in the case of the 1OH3C3 would involve the formation of the $(O_2NO–C_3H_6)–O^+$ at m/z 120 and $(O_2NO–C_3H_6)^+$ at m/z 104, but their spectral signature is marginal into the spectra.

As expected, the intensity of the signal 43 increases with increasing E/N ratio. The opposite tendency was observed for adducts. The mass spectrum obtained at $E/N^* = 41$, which corresponds to the highest sensitivity for the m/z 151 signal, is shown in Fig. 5b.

Besides the abovementioned characteristic signals, other specific mechanisms could be associated to the spectral signature of 1OH3C3. The mechanism is reviewed and suggested by Harrison (1999) for the particular case of NO^+ ionization of primary alcohols. In this study, an additional product ($R(–2H) + NO^+$) has been observed which would correspond in our case to an $m/z = 149$, hypothetically formed by the oxidation of the alcohol to the corresponding aldehyde and its subsequent ionization. Although relatively weak, the signal is systematically recorded in the mass spectra of the hydroxynitrate. The 45 and 67 ions are equally present in mass spectra and can be attributed to fragmentation.

The detection limit obtained in NO^+ ionization mode at E/N ratio of 41 Td* for the $M \cdot NO^+$ signal at m/z 151 was quite low (37 ppt min^{-1}), showing that this ionization mode is more suitable than H_3O^+ mode for the measurement of hydroxynitrates. As shown in Table 2, the hydrogen abstraction signal (m/z 120) is at least 1 order of magnitude less sensitive.

3.4 Ketonitrates

3.4.1 The H_3O^+ ionization

Two distinct ketonitrates were synthesized and characterized in the current study: 3-nitroxy-2-propanone (KnC3) and the 3-nitroxy-3-methyl-2-butanone (KnC5).

In order to identify the optimal conditions for the detection of ketonitrates in H_3O^+ ionization mode, tests were performed by varying E/N ratios into a large domain, from 45 to 170 Td (Fig. 6).

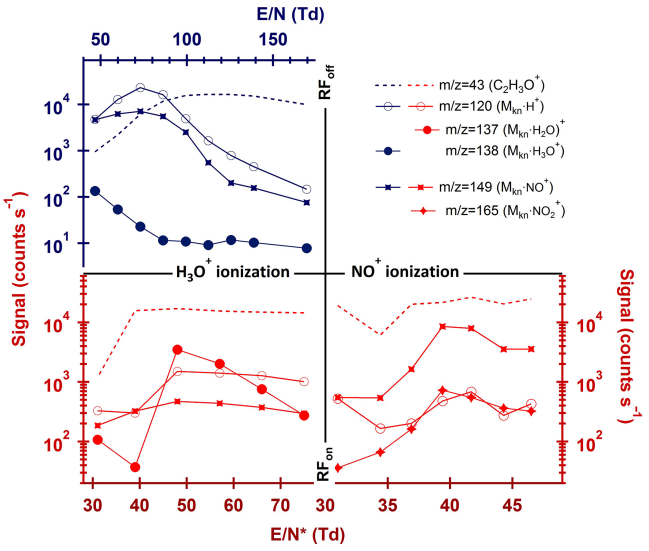

Figure 6. The E/N ratio influence over the KnC3 identification for several representative signals in both ionization modes (H_3O^+, left; NO^+, right) as recorded in absence (up)/presence (down) of a RF funnel. The common signal at $m/z = 43$ is equally plotted as a fragmentation mark (right axis).

Several signals which can be attributed to ketonitrates have been detected, as illustrated in Fig. 6 for KnC3: at low E/N ratios, which correspond to the $H_3O^+(H_2O)_2$ controlled regime, the formation of two ketonitrate water cluster adducts, $M_{kn} \cdot H_3O^+$ ($m/z = 138$) and $M_{kn} \cdot H_3O^+(H_2O)$ ($m/z = 156$), has been observed. It is worth noting the reduction of these specific signals with the decay of the preeminent ionizing analyte $H_3O^+(H_2O)_2$ ($m/z = 55$) signal. With the data available in literature we expect that for polar compounds the ionization process may follow two similar pathways: by proton transfer (Reaction R9a) and by ligand-switching reaction (Reaction R9b) (de Gouw et al., 2003).

$$M_{kn} + H_3O^+(H_2O)_n \rightarrow M_{kn}H^+ + (n+1)H_2O \quad \text{(R8a)}$$

$$M_{kn} + H_3O^+(H_2O)_n \rightarrow M_{kn}H^+(H_2O)_m + (n-m+1)H_2O \quad \text{(R8b)}$$

The bound energy of the cluster ions formed in the reaction above (Reaction R9b) is weaker than the water cluster bond. In the given conditions, there is a high probability that the drift tube dissociative effect can split the formed cluster ions and lead to the formation of MH^+ and $MH^+ \cdot (H_2O)$. Since the cluster ion distribution may be governed by the water vapor drift tube loads, the detection efficiency can be reliant on humidity in this particular case (de Gouw et al., 2003).

Redistribution processes among the various precursor ions formed into the glow discharge can equally occur, leading to the formation of auxiliary hydrated ions such as $NO^+(H_2O)_n$, able to produce ligand-switching reactions similar to the ones presented above (Reaction R9b).

For intermediate E/N ratios, where $H_3O^+(H_2O)$ water cluster is the key analyte, we notice that the signal corresponding to $M_{kn}\cdot H^+$ ($m/z = 120$) is maximum. In addition, two other signals corresponding to $M_{kn}\cdot NO^+$ ($m/z = 149$) and $M_{kn}\cdot NO_2^+$ ($m/z = 165$) adduct formation have also been observed and rise up to a maximum for these intermediate E/N ratios. These adducts can be explained by the formation of NO^+ and NO_2^+ analytes in the GD, which increases with the increasing E/N ratios.

For high E/N ratios, the m/z 43 ($C_2H_3O^+$) signal, which is a common fragment of organic compounds, strongly increases. This reveals that mainly fragmentation occurs, making this region unsuitable for the detection of ketonitrates.

From these results, the intermediate E/N ratios (70–80 Td) appear to be the most suitable for the detection of ketonitrates in H_3O^+ ionization mode. Mass spectra obtained at $E/N = 75$ Td, which corresponds to the highest sensitivity of the $M_{kn}\cdot H^+$ signal, are shown in Fig. 7 for KnC3 and in Fig. S4 for KnC5 respectively.

For KnC3, the most intense signal corresponds to $M_{kn}\cdot H^+$ ($m/z = 120$). As discussed above, additional processes occur which are responsible for other signals: $M_{kn}\cdot NO^+$ adduct formation at m/z 149 and fragmentation at m/z 43 ($C_2H_3O^+$). These characteristic signals are tailed by their corresponding isotopic abundance signals mainly due to ^{13}C isotope at $m/z = 121$ and 150.

The already discussed Reactions (R5) and (R6) could explain the intense signal of m/z 75 since the resulting (C_3H_5O)–$OH\cdot H^+$ ion seems the accurate match of this signal.

It is worth noting that due to the low E/N ratios, imposed by the breakability of organic nitrates, in the above illustrated mass spectra examples, the intensities of the signals m/z 19 (H_3O^+) and 37 ($H_3O^+(H_2O)$) are of the same order of magnitude while the m/z 55 ($H_3O^+(H_2O)_2$) is 1 or 2 orders of magnitude lower.

In the case of KnC5, the $M_{kn}\cdot H^+$ ($m/z = 148$) signal is not the most intense one, suggesting that fragmentation is more favored that for KnC3 under similar conditions. The characteristic fragmentation pattern of this analyte exhibits a characteristic m/z 85 signal corresponding to the $C_5H_9O^+$ group after the cleavage of the NO_3 fragment. An analogous process is described by Aoki et al. (2007), asserting the alkyl group as the main signal in the mass spectra of alkyl nitrates. The abundant m/z 59 fragment ($C_3H_7O^+$ or $C_2H_3O_2^+$) is most probably a result of subsequent fragmentation/recombination processes.

The intense $m/z = 103$ signal could be ascribed to the already mentioned Reactions (R5) and/or (R6), both conducting to the formation of a (C_5H_9O)–$OH\cdot H^+$ ion with release of HNO_3 and water. It is worth noting that the elimination of supplementary H_2O from the resulting complex could also contribute to the m/z 85 signal ($C_5H_9O^+$).

In the RF mode, the water cluster distribution is dominated by the H_3O^+ ion, for the entire range of E/N^* ratios. Its signal is the most abundant, while all the other $H_3O^+(H_2O)_n$ species are at least 1 order of magnitude lower. The redistribution of water cluster in the RF mode modifies obviously the ketonitrates' fragmentation pattern and the burden of each ionization channel in a similar way as in the case of hydroxynitrates. No straightforward correlation can be made in between the two modes, showing the complexity of the ion funnel influence.

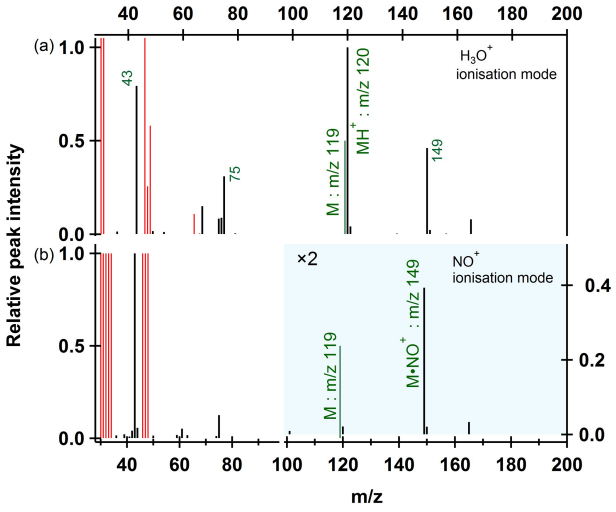

Figure 7. Recorded mass spectrum of protonated KnC3 (black bars) for $E/N = 75$ Td, corresponding to the highest sensitivity for the protonated analyte signal detection (m/z 120) in absence of the RF device **(a)** and in the NO^+ ionization mode in presence of the RF ($E/N^* = 40$ Td) **(b)**. The thin green line represents the expected molecular ion of the analyte. The intense signals depicted by the red thin bars represent the ionizing and matrix analytes at $m/z = 30$ (NO^+) and 46 (NO_2^+) and their isotopic abundance signals at $m/z = 31$ and 47, 48 respectively. The signals corresponding to the water clusters $(H_3O^+(H_2O)_n$ at m/z 37 and 55 are systematically erased for simplification.

The most noteworthy difference in the RF mode resides in the presence of an intense signal corresponding to a H_2O adduct formation (m/z 137 and 165 respectively), similar to the hydroxynitrate, with a maximum intensity around 48 Td (Table 2) as calculated without taking into account the RF contribution.

With the same PTR entry voltage, the RF mode activation induces the enhancement of the fragmentation due to higher input energies and the maximum of the protonated ketonitrate signal glides towards 48 Td. Making the assumption that the highest sensitivity is related in the two modes to an analogous E/N state, a coarse assessment of the RF mode contribution is estimated (25–35 Td) as the difference between the two modes maximum sensitivity for the protonated molecular ion signal.

To conclude, it has been observed that protonation of ketonitrates is the main ionization process in the absence of a RF field. The use of the RF mode modifies the fragmen-

tation pattern and enhances the mechanism, leading to the $M \cdot H_2O^+$ adduct formation. The recorded sensitivities listed in Table 2 for the H_3O^+ ionization mode are corresponding to a DL of 70–80 ppt min^{-1} for the protonated signal of KnC3 (m/z 120). A similar DL is reached by the water adduct signal at m/z 137 under the influence of the RF ion funnel. The highest sensitivity for the KnC5 identification is attained by the water adduct signal at m/z 165 recorded at 48 Td in the RF mode with a DL of 20 ppt min^{-1}. Sensitivities of other specific signals are equally proposed for comparison in Table 2.

3.4.2 The NO^+ ionization

For the first time, the detection of ketonitrates using NO^+ ionization was tested. In a similar way as for the protonation process, mass spectra of KnC3 and KnC5 were recorded as a function of E/N ratios. The previously proven affinity of NO^+ coupling –C(O) functional group in ketones to form adducts (Smith et al., 2003) was for the first time tested in a PTR reactor. The adduct formation was successfully achieved in the presence of NO^+ for both studied ketonitrates, for which very similar IE are expected.

In the given ionization mode and considering the higher IE of ketonitrates, the adduct formation is expected to prevail over the charge transfer, the literature stating that the yield of parent radical cation formation seems to be anticorrelated with the IE of the ketones, the lowest IE analytes, presenting the highest probability for the charge transfer reaction (Smith et al., 2003).

Following the same approach as in the previous case, the E/N^* region was set in order to provide the highest NO^+/NO_2^+ ratio. Figures 6 and S5 present the influence of the E/N ratio variation in the RF mode over the analyte signal of interest. We notice that the quick enhancement of the NO^+/NO_2^+ ratio is accompanied by the adduct signal increase.

We plot as an example, the KnC5 adduct signal at m/z = 177 (147 + 30) as a function of two fragments (m/z = 43 and 85) with potentially, as explained above, different formation pathways. A decrease of the fragmentation yield in favor of the adduct formation in the PTR reactor is observed over the 35 Td shoulder. The high sensitivity of the instrumental setup for the identification of ketonitrates is quantified in Table 2.

Due to the rising incidence of the NO^+ and NO_2^+ ions, simultaneously formed in the GD, the signals corresponding to the $M_{kn} \cdot NO^+$ and $M_{kn} \cdot NO_2^+$ adduct formation are equally strengthened (m/z = 149 and 165 for the KnC3 and m/z = 177 and 193 for the KnC5; see Figs. 7b and S4 respectively). All these characteristic signals are tailed by their corresponding isotopic abundance signals due mainly to ^{13}C isotope at m/z = 121, 150, 166, 178 and 194.

The KnC3 spectrum was recorded at E/N^* = 40 Td as shown in Fig. 7b. We notice a low fragmentation pattern of the analyte with a major adduct signal contribution at m/z = 149. The existence of a secondary (water-controlled) competitive process might be revealed by the existence of the minor protonated signal at m/z 120 backed by the characteristic fragment at m/z = 75 as described by Reactions (R5)–(R7).

In an analog way, in Fig. S4, the mass spectrum of KnC5 is plotted for the instrumental setup corresponding at the lowest fragmentation (E/N^* = 36 Td). We notice the distinct signal of the formed adduct (m/z = 177) as well as, to a lesser extent, the characteristic signals described above (m/z = 59, 85, 103), which are most likely formed following the mechanisms described in the previous paragraph, since the water is ubiquitously present in the system.

The best results of the NO^+ ionization are related typically to the highest NO^+/NO_2^+ ratios in the RF mode as seen in Table 2. The NO^+ high affinity towards adduct formation is confirmed by the low DL achieved for these highly characteristic signals: 30 and 40 ppt min^{-1} for the adducts formed at m/z 149 and 177, respectively, at an E/N^* ratio < 45 Td.

3.5 PANs

The detection of PANs with PTR-MS has been tested by generating the PAN from the well-known NO_3 oxidation of acetaldehyde in the simulation chamber. The disadvantage of this procedure despite the 70 % PAN formation yield (Doussin et al., 2003) is that it generates several bi-products (nitric acid, formaldehyde, etc.) leading to more complex mass spectra. The PAN family analytes were all obtained by in situ generation using the corresponding aldehydes. In order to overcome any judgment error, the present study will only illustrate the PAN mass spectra while for the other analogous formed PAN-like products (P2MCrN and P3MCrN) we will only discuss the mass spectra signals which are assigned to them.

3.5.1 The H_3O^+ ionization

The optimal conditions for the detection of PANs in H_3O^+ ionization mode were explored by varying the E/N ratios from 55 to 120 Td. The most promising results were obtained in the case of PAN around 85 Td, where the protonated signal of PAN was recorded as we can depict from Fig. S6.

In a manner analogous to the Reaction (R1a), the protonated peroxynitrates are equally expected to form low energy gas-phase ion-dipole complexes ($ROOH \cdot NO_2^+$) with bound energies of 92 kJ mol^{-1} in the case of methyl-peroxynitrate (Ravelo and Francisco, 2007). Previous studies (Hansel and Wisthaler, 2000) have proposed a speculative decomposition of the protonated PAN:

$$RC(O)OONO_2H^+ + H_2O \rightarrow RC(O)OOHH^+ + HNO_3. \quad \text{(R9)}$$

The same mechanism is equally indicated by later studies (Aoki et al., 2007), giving the mass spectral signal at m/z =

77, as recorded in the case of the PAN (Fig. S6). According to their statements the other protonated PAN parent compound generated in our study (C_4H_7-C(O)OONO$_2$H$^+$, $m/z = 162$) should lead to representative ionic signals of type C_4H_7-C(O)OOHH$^+$, $m/z = 117$, which are indeed present in the deconvoluted mass spectra of our analytes. Moreover, the fact that this signal is absent during the NO^+ ionization mode (characterized by inferior H_2O levels) may support this hypothetic decomposition of the PANs.

Another likely mechanism which, unexpectedly, may lead to the same analytical signal is reviewed by Roberts (1990), proposing the unimolecular decomposition of PANs to form the corresponding C_{n-1} alkyl nitrate. In our particular case the reaction may be written as

$$C_4H_7\text{-C(O)OONO}_2 \rightarrow C_4H_7\text{-ONO}_2 + CO_2. \quad \text{(R10)}$$

Assuming the presence of both processes, the resulting alkyl nitrate may interfere with the abovementioned $m/z = 117$ signal in the case of a charge transfer reaction. More likely, in the case of a protonation process, the obtained $m/z = 118$ signal derived from the alkyl nitrate will enhance the isobaric signal due to the ^{13}C isotopic abundance of the analyte obtained by PAN decomposition. The signal of m/z 118 seems indicative of the presence of a double peak which might confirm the occurrence of both processes. This fact is equally confirmed by the I_{118}/I_{117} measured ratio (0.19–0.23 for the P2MCrN and 0.52–0.57 for the P3MCrN), which is significantly different from the expected ^{13}C isotopic abundance for a RC(O)OOHH$^+$-type compound (0.06). This difference suggests the presence of this kind of analytical interference, more pronounced in the case of P3MCrN.

However the PAN decomposition path is considered to be several hundred times slower than the bond homolysis channel:

$$C_4H_7\text{–C(O)OONO}_2 \rightarrow C_4H_7\text{–C(O)OO}^{\cdot} + NO_2. \quad \text{(R11)}$$

The recombination of C_4H_7–C(O)OO$^{\cdot}$ ($m/z = 115$) with highly abundant $H^+(H_2O)$ and $H^+(H_2O)_2$ could generate the signals at m/z 133 and 151 respectively. Additionally, the high levels of NO_2^+ ($m/z = 46$) may favor the presence of $NO_2^+ \cdot H_2O$ ($m/z = 64$), which can potentially quench the C_4H_7–C(O)OO$^{\cdot}$ radical to give an adduct signal at $m/z =$ 179.

In order to certify the mono-nitrogen-containing analytes for several ion signals in the spectrum, an analysis similar to the one performed by Inomata et al. (2013), which consists of subtraction of the isotopic effect of ^{13}C by calculating I_{even}/I_{odd} ratios of an ion signal at an even m/z [M] to the adjacent ion signal at an odd m/z [M + 1], was performed.

As described by Table 2 the normalized sensitivity for the protonated PANs is weak, spanning few counts of ppb^{-1} min^{-1} for all three considered PANs.

3.5.2 The NO^+ ionization

Unlike the ketonitrates, the PANs present a low sensitivity towards detection in NO^+ ionization mode and generally a complex chemical equilibrium in classical PTR analysis.

In the NO^+ ionization mode, the signals corresponding to adduct formation are barely noticeable for the entire range of E/N considered. However, the presence of weak signals at $m/z = 191$ and 207 for both P2MCrN and P3MCrN is indicative of the presence of PAN NO^+ and PAN NO_2^+ adducts respectively.

The thermolability of the PANs was equally considered for the weak response factors of the instrumental setup in both ionization modes, since the sampling requires slightly heated inlet lines. We considered the 40 °C heating as a compromise between the thermolability of the organic nitrates and the risk of condensation in the sampling line. However, the total residence in the sampling line and the instrument inlet is very short, around 3s. At 40 °C, the lifetime of PAN (due to thermal decomposition) is around 300 s. So decomposition of PANs is expected to be negligible here.

4 Conclusions

Organic nitrates play a key role in atmospheric chemistry as they act as reactive nitrogen reservoir species. The use of PTR-MS for the measurement of volatile organic compounds has expanded a lot in atmospheric research these last years but few studies have investigated the performances of this instrument for the detection of organic nitrates. These studies have shown that this technique exhibits poor performances (high fragmentation and poor sensitivity) when it is run in classical mode.

In the present work, the detection of alkyl and multifunctional organic nitrates (PANs, ketonitrates, hydroxynitrates) by this technique has been studied by operating the instrument in the classical mode (H_3O^+ as ionizing species) but also by testing an NO^+-induced, soft ionization. The versatility of the instrument allows an easy change of the chemical ionization source from H_3O^+ to NO^+ by simply replacing water vapor by dry air in the glow discharge. This is very useful for a double identification of the organic nitrates.

This study has shown that two complementary ionization modes can be used for the detection of organic nitrates:

- The NO^+ ionization mode in presence of RF mode with an E/N ratio around 45Td is our first choice. This mode favors the M–NO^+ adduct formation and has been shown to be more efficient for the detection of all types of organic nitrates except PANs (i.e., alkyl, hydroxynitrates and carbonyl nitrates), as it minimizes fragmentation, favoring the identification of molecular composition. In addition, this mode is much more sensitive to the detection of hydroxy- and ketonitrates than the pro-

tonation one. Thus, we recommend the use of this mode for alkyl and multifunctional organic nitrates.

– The protonation mode in absence of the RF mode, for an E/N ratio around 70Td which is recommended for the detection of PAN-type compounds is our second choice. This ionization mode can also be used for other types of organic nitrates but with lower sensitivity than the NO^+ mode.

Although slight variations appear in the optimization of the operational conditions for each type of compounds, it has been observed that a few unit shifts of the E/N ratios do not significantly affect the analytical sensitivity of the method. The NO^+ adduct ionization mode appears to be the most sensitive for the detection of hydroxy- and ketonitrates with detection limits in the range of tens of ppt/min. This high sensitivity is suitable for the detection of organic nitrates in lab studies, in particular in simulation chamber experiments. It also suggests that this method is very promising for the detection of these compounds in ambient air. The detection of alkyl nitrates and PANs with PTR-MS is less sensitive, with detection limits in the range of hundreds ppt of min^{-1}, whatever the ionization source used.

From this study, we now better understand how to run PTR-MS to allow the detection of individual organic nitrates during lab studies and this will be very useful for a number of research groups working on mechanisms studies which are equipped with this instrument. In particular, the operational mode of the instrument has been optimized for the detection of different types of organic nitrates and the ionization pattern (fragmentation, adduct formation, charge transfer, etc.) of these species is much better understood now.

A perspective of this work was to test the detection of organic nitrates in ambient air with this method. From the detection limits observed in this study, we can expect that accumulations over longer periods will be necessary to decrease the detection limits.

A crucial aspect to be taken into account in further studies for lab and field measurements using this method is the effect of the humidity of the sampled air. In addition, longer acquisition time, elimination of interfering ionization paths by selective ionization sources and softer ionization sources could improve the technique's performance.

Data availability. Data available upon request.

The Supplement related to this article is available online at doi:10.5194/amt-10-1445-2017-supplement.

Competing interests. The authors declare that they have no conflict of interest.

Acknowledgements. This work was supported by the French National Agency for Research (Project ONCEM-ANR-12-BS06-0017-01), by the European Union's Horizon 2020 research and innovation programme through the EUROCHAMP-2020 Infrastructure Activity under grant agreement no. 730997 and by the Région Ile de France. The authors also thank Fraiser Reich and Kore Company for their advices in the use of the PTR-MS.

Edited by: D. Heard
Reviewed by: two anonymous referees

References

Allen, G., Remedios, J. J., Newnham, D. A., Smith, K. M., and Monks, P. S.: Improved mid-infrared cross-sections for peroxyacetyl nitrate (PAN) vapour, Atmos. Chem. Phys., 5, 47–56, doi:10.5194/acp-5-47-2005, 2005.

Amadei, G. and Ross, B. M.: The reactions of a series of terpenoids with H_3O^+, NO^+ and O_2^+ studied using selected ion flow tube mass spectrometry, Rapid Commun. Mass Sp., 25, 162–168, 2011.

Aoki, N., Inomata, S., and Tanimoto, H.: Detection of C_1-C_5 alkyl nitrates by proton transfer reaction time-of-flight mass spectrometry, Int. J. Mass Spectrom., 263, 12–21, 2007.

Arey, J., Aschmann, S. M., Kwok, E. S. C., and Atkinson, R.: Alkyl nitrate, hydroxyalkyl nitrate, and hydroxycarbonyl formation from the NO_x – air photooxidations of C_5–C_8 n-alkanes, J. Phys. Chem. A, 105, 1020–1027, 2001.

Atkinson, R.: Atmospheric chemistry of VOCs and NO_x, Atmos. Environ., 34, 2063–2101, 2000.

Atlas, E.: Evidence for $=C_3$ alkyl nitrates in rural and remote atmospheres, Nature, 331, 426–428, 1988.

Barber, S., Blake, R. S., White, I. R., Monks, P. S., Reich, F., Mullock, S., and Ellis, A. M.: Increased sensitivity in Proton Transfer Reaction Mass Spectrometry by incorporation of a radio frequency ion funnel, Anal. Chem., 84, 5387–5391, 2012.

Barnes, I., Bastian, V., Becker, K. H., and Tong, Z.: Kinetics and products of the reactions of nitrate radical with monoalkenes, dialkenes, and monoterpenes, J. Phys. Chem., 94, 2413–2419, 1990.

Bates, K. H., Crounse, J. D., St. Clair, J. M., Bennett, N. B., Nguyen, T. B., Seinfeld, J. H., Stoltz, B. M., and Wennberg, P. O.: Gas phase production and loss of isoprene epoxydiols, J. Phys. Chem. A, 118, 1237–1246, 2014.

Baughman, T. W., Sworen, J. C., and Wagener, K. B.: The facile preparation of alkenyl metathesis synthons, Tetrahedron, 60, 10943–10948, 2004.

Beaver, M. R., Clair, J. M. St., Paulot, F., Spencer, K. M., Crounse, J. D., LaFranchi, B. W., Min, K. E., Pusede, S. E., Wooldridge, P. J., Schade, G. W., Park, C., Cohen, R. C., and Wennberg, P. O.: Importance of biogenic precursors to the budget of organic nitrates: observations of multifunctional organic nitrates by CIMS and TD-LIF during BEARPEX 2009, Atmos. Chem. Phys., 12, 5773–5785, doi:10.5194/acp-12-5773-2012, 2012.

Berndt, T. and Böge, O.: Products and mechanism of the reaction of NO_3 with selected acyclic monoalkenes, J. Atmos. Chem., 21, 275–291, 1995.

Blake, N. J., Blake, D. R., Wingenter, O. W., Sive, B. C., Kang, C. H., Thornton, D. C., Bandy, A. R., Atlas, E., Flocke, F., Harris, J. M., and Rowland, F. S.: Aircraft measurements of the latitudinal, vertical, and seasonal variations of NMHCs, methyl nitrate, methyl halides, and DMS during the First Aerosol Characterization Experiment (ACE 1), J. Geophys. Res.-Atmos., 104, 21803–21817, 1999.

Blake, R. S., Monks, P. S., and Ellis, A. M.: Proton-Transfer Reaction Mass Spectrometry, Chem. Rev., 109, 861–896, 2009.

Browne, E. C., Min, K.-E., Wooldridge, P. J., Apel, E., Blake, D. R., Brune, W. H., Cantrell, C. A., Cubison, M. J., Diskin, G. S., Jimenez, J. L., Weinheimer, A. J., Wennberg, P. O., Wisthaler, A., and Cohen, R. C.: Observations of total $RONO_2$ over the boreal forest: NO_x sinks and HNO_3 sources, Atmos. Chem. Phys., 13, 4543–4562, doi:10.5194/acp-13-4543-2013, 2013.

Buhr, M. P., Parrish, D. D., Norton, R. B., Fehsenfeld, F. C., Sievers, R. E., and Roberts, J. M.: Contribution of organic nitrates to the total reactive nitrogen budget at a rural eastern U.S. site, J. Geophys. Res.-Atmos., 95, 9809–9816, 1990.

Cacace, F. and de Petris, G.: Mass spectrometric study of simple main group molecules and ions important in atmospheric processes, Int. J. Mass Spectrom., 194, 1–10, 2000.

Cacace, F., de Petris, G., and Pepi, F.: Gas-phase NO^+ affinities, P. Natl. Acad Sci. USA, 94, 3507–3512, 1997.

Castedo, L., Marcos, C. F., Monteagudo, M., and Tojo, G.: New one-pot synthesis of alkyl nitrates from alcohols, Synthetic Commun., 22, 677–681, 1992.

Curci, G., Beekmann, M., Vautard, R., Smiatek, G., Steinbrecher, R., Theloke, J., and Friedrich, R.: Modelling study of the impact of isoprene and terpene biogenic emissions on European ozone levels, Atmos. Environ., 43, 1444–1455, 2009.

D'Anna, B., Wisthaler, A., Andreasen, Ø., Hansel, A., Hjorth, J., Jensen, N. R., Nielsen, C. J., Stenstrøm, Y., and Viidanoja, J.: Atmospheric chemistry of C3-C6 cycloalkanecarbaldehydes, J. Phys. Chem. A, 109, 5104–5118, 2005.

Day, D. A., Wooldridge, P. J., Dillon, M. B., Thornton, J. A., and Cohen, R. C.: A thermal dissociation laser-induced fluorescence instrument for in situ detection of NO_2, peroxy nitrates, alkyl nitrates, and HNO_3, J. Geophys. Res.-Atmos., 107, 5–6, 2002.

de Gouw, J. and Warneke, C.: Measurements of volatile organic compounds in the earths atmosphere using proton-transfer-reaction mass spectrometry, Mass Spectrom. Rev., 26, 223–257, 2007.

de Gouw, J., Warneke, C., Karl, T., Eerdekens, G., van der Veen, C., and Fall, R.: Sensitivity and specificity of atmospheric trace gas detection by proton-transfer-reaction mass spectrometry, Int. J. Mass Spectrom., 223–224, 365–382, 2003.

De Laeter, J. R., Böhlke, J. K., De Bièvre, P., Hidaka, H., Peiser, H. S., Rosman, K. J. R., and Taylor, P. D. P.: Atomic weights of the elements: Review 2000 (IUPAC Technical Report), Pure Appl. Chem., 75, 683–800, 2003.

Diskin, A. M., Wang, T., Smith, D., and Španěl, P.: A selected ion flow tube (SIFT), study of the reactions of H_3O^+, NO^+ and O_2^+ ions with a series of alkenes; in support of SIFT-MS, Int. J. Mass Spectrom., 218, 87–101, 2002.

Doussin, J. F., Picquet-Varrault, B., Durand-Jolibois, R., Loirat, H., and Carlier, P.: A visible and FTIR spectrometric study of the nighttime chemistry of acetaldehyde and PAN under simulated atmospheric conditions, J. Photoch. Photobio. A, 157, 283–293, 2003.

Fischer, R., Weller, R., Jacobi, H.-W., and Ballschmiter, K.: Levels and pattern of volatile organic nitrates and halocarbons in the air at Neumayer Station (70° S), Antarctic, Chemosphere, 48, 981–992, 2002.

Fischer, R. G., Kastler, J., and Ballschmiter, K.: Levels and pattern of alkyl nitrates, multifunctional alkyl nitrates, and halocarbons in the air over the Atlantic Ocean, J. Geophys. Res.-Atmos., 105, 14473–14494, 2000.

Flocke, F., Volz-Thomas, A., and Kley, D.: Measurements of alkyl nitrates in rural and polluted air masses, Atmos. Environ. A-Gen., 25, 1951–1960, 1991.

Flocke, F. M., Weinheimer, A. J., Swanson, A. L., Roberts, J. M., Schmitt, R., and Shertz, S.: On the measurement of PANs by gas chromatography and electron capture detection, J. Atmos. Chem., 52, 19–43, 2005.

Francisco, M. A. and Krylowski, J.: Chemistry of organic nitrates: thermal chemistry of linear and branched organic nitrates, Ind. Eng. Chem. Res., 44, 5439–5446, 2005.

Fukui, Y. and Doskey, P. V.: A measurement technique for organic nitrates and halocarbons in ambient air, J. High Res. Chromatog., 21, 201–208, 1998.

Gaffney, J. S., Marley, N. A., Steele, H. D., Drayton, P. J., and Hubbe, J. M.: Aircraft measurements of nitrogen dioxide and peroxyacyl nitrates using luminol chemiluminescence with fast capillary gas chromatography, Environ. Sci. Technol., 33, 3285–3289, 1999.

Goebbert, D. and Wentold, P.: Water dimer proton affinity from the kinetic method: dissociation energy of the water dimer, Eur. J. Mass Spectrom., 10, 837–846, 2004.

Grosjean, D. and Harrison, J.: Peroxyacetyl nitrate – comparison of alkaline-hydrolysis and chemi-luminescence methods, Environ. Sci. Technol., 19, 749–752, 1985.

Hansel, A. and Wisthaler, A.: A method for real-time detection of PAN, PPN and MPAN in ambient air, Geophys. Res. Lett., 27, 895–898, 2000.

Hanst, P. L.: Mechanism of peroxyacetyl nitrate formation, JAPCA J. Air Waste Ma., 21, 269–271, 1971.

Hao, C., Shepson, B., Drummond, J. W., and Muthuramu, K.: Gas chromatographic detector for selective and sensitive detection of atmospheric organic nitrates, Anal. Chem., 66, 3737–3743, 1994.

Harrison, A. G.: Chemical Ionization in Mass Spectrometry*, in: Encyclopedia of Spectroscopy and Spectrometry (2nd edition), edited by: Lindon, J. C., Academic Press, Oxford, UK, 1999.

Hewitt, C. N., Hayward, S., and Tani, A.: The application of proton transfer reaction-mass spectrometry (PTR-MS) to the monitoring and analysis of volatile organic compounds in the atmosphere, J. Environ. Monitor., 5, 1–7, 2003.

Horowitz, L. W., Fiore, A. M., Milly, G. P., Cohen, R. C., Perring, A., Wooldridge, P. J., Hess, P. G., Emmons, L. K., and Lamarque, J. F.: Observational constraints on the chemistry of isoprene nitrates over the eastern United States, J. Geophys. Res.-Atmos., 112, D12S08, doi:10.1029/2006JD007747, 2007.

Huey, L. G.: Measurement of trace atmospheric species by chemical ionization mass spectrometry: Speciation of reactive nitrogen and future directions, Mass Spectrom. Rev., 26, 166–184, 2007.

Hunter, E. P. L. and Lias, S. G.: Evaluated gas phase basicities and proton affinities of molecules: An update, J. Phys. Chem. Ref. Data, 27, 413–656, 1998.

Iachetta, L., Malek, L., and Ross, B. M.: The reactions of H_3O^+, NO^+ and O_2^+ with several flavourant esters studied using selected ion flow tube mass spectrometry, Rapid Commun. Mass Sp., 24, 815–822, 2010.

Inomata, S., Tanimoto, H., Fujitani, Y., Sekimoto, K., Sato, K., Fushimi, A., Yamada, H., Hori, S., Kumazawa, Y., Shimono, A., and Hikida, T.: On-line measurements of gaseous nitro-organic compounds in diesel vehicle exhaust by proton-transfer-reaction mass spectrometry, Atmos. Environ., 73, 195–203, 2013.

Jacobs, M. I., Burke, W. J., and Elrod, M. J.: Kinetics of the reactions of isoprene-derived hydroxynitrates: gas phase epoxide formation and solution phase hydrolysis, Atmos. Chem. Phys., 14, 8933–8946, doi:10.5194/acp-14-8933-2014, 2014.

Kames, J., Schurath, U., Flocke, F., and Volz-Thomas, A.: Preparation of organic nitrates from alcohols and N_2O_5 for species identification in atmospheric samples, J. Atmos. Chem., 16, 349–359, 1993.

Karl, T., Hansel, A., Cappellin, L., Kaser, L., Herdlinger-Blatt, I., and Jud, W.: Selective measurements of isoprene and 2-methyl-3-buten-2-ol based on NO^+ ionization mass spectrometry, Atmos. Chem. Phys., 12, 11877–11884, doi:10.5194/acp-12-11877-2012, 2012.

Kastler, J. and Ballschmiter, K.: Identification of alkyl dinitrates in ambient air of Central Europe, Fresen. J. Anal. Chem., 363, 1–4, 1999.

Knighton, W. B., Fortner, E. C., Herndon, S. C., Wood, E. C., and Miake-Lye, R. C.: Adaptation of a proton transfer reaction mass spectrometer instrument to employ NO^+ as reagent ion for the detection of 1,3-butadiene in the ambient atmosphere, Rapid Commun. Mass Sp., 23, 3301–3308, 2009.

Kriemler, P. and Buttrill, S. E.: Positive and negative ion-molecule reactions and the proton affinity of ethyl nitrate, J. Am. Chem. Soc., 92, 1123–1128, 1970.

Lee, B. H., Lopez-Hilfiker, F. D., Mohr, C., Kurtén, T., Worsnop, D. R., and Thornton, J. A.: An iodide-adduct high-resolution time-of-flight chemical-ionization mass spectrometer: Application to atmospheric inorganic and organic compounds, Environm. Sci. Technol., 48, 6309–6317, 2014.

Lee, T. J. and Rice, J. E.: Proton affinity of methyl nitrate: less than proton affinity of nitric acid, J. Am. Chem. Soc., 114, 8247–8256, 1992.

Luxenhofer, O. and Ballschmiter, K.: C4–C14-alkyl nitrates as organic trace compounds in air, Fresen. J. Anal. Chem., 350, 395–402, 1994.

Luxenhofer, O., Schneider, E., and Ballschmiter, K.: Separation, detection and occurrence of (C2–C8)-alkyl- and phenyl-alkyl nitrates as trace compounds in clean and polluted air, Fresen. J. Anal. Chem., 350, 384–394, 1994.

Madronich, S. and Calvert, J. G.: Permutation reactions of organic peroxy radicals in the troposphere, J. Geophys. Res., 95, 5697–5715, 1990.

Mills, G. P., Hiatt-Gipson, G. D., Bew, S. P., and Reeves, C. E.: Measurement of isoprene nitrates by GCMS, Atmos. Meas. Tech., 9, 4533–4545, doi:10.5194/amt-9-4533-2016, 2016.

Mochalski, P., Unterkofler, K., Španěl, P., Smith, D., and Amann, A.: Product ion distributions for the reactions of NO^+ with some physiologically significant aldehydes obtained using a SRI-TOF-MS instrument, Int. J. Mass Spectrom., 363, 23–31, 2014.

Müller, M., Graus, M., Wisthaler, A., Hansel, A., Metzger, A., Dommen, J., and Baltensperger, U.: Analysis of high mass resolution PTR-TOF mass spectra from 1,3,5-trimethylbenzene (TMB) environmental chamber experiments, Atmos. Chem. Phys., 12, 829–843, doi:10.5194/acp-12-829-2012, 2012.

Muthuramu, K., Shepson, P. B., and O'Brien, J. M.: Preparation, analysis, and atmospheric production of multifunctional organic nitrates, Environ. Sci. Technol., 27, 1117–1124, 1993.

O'Brien, J. M., Shepson, P. B., Muthuramu, K., Hao, C., Niki, H., Hastie, D. R., Taylor, R., and Roussel, P. B.: Measurements of alkyl and multifunctional organic nitrates at a rural site in Ontario, J. Geophys. Res.-Atmos., 100, 22795–22804, 1995.

Paul, D., Furgeson, A., and Osthoff, H. D.: Measurements of total peroxy and alkyl nitrate abundances in laboratory-generated gas samples by thermal dissociation cavity ring-down spectroscopy, Rev. Sci. Instrum., 80, 114101, doi:10.1063/1.3258204, 2009.

Perraud, V., Bruns, E. A., Ezell, M. J., Johnson, S. N., Greaves, J., and Finlayson-Pitts, B. J.: Identification of Organic Nitrates in the NO_3 Radical Initiated Oxidation of alpha-Pinene by Atmospheric Pressure Chemical Ionization Mass Spectrometry, Environ. Sci. Technol., 44, 5887–5893, 2010.

Perring, A. E., Bertram, T. H., Farmer, D. K., Wooldridge, P. J., Dibb, J., Blake, N. J., Blake, D. R., Singh, H. B., Fuelberg, H., Diskin, G., Sachse, G., and Cohen, R. C.: The production and persistence of $\Sigma RONO_2$ in the Mexico City plume, Atmos. Chem. Phys., 10, 7215–7229, doi:10.5194/acp-10-7215-2010, 2010.

Ravelo, R. M. and Francisco, J. S.: Proton Affinity of Methyl Peroxynitrate, J. Phys. Chem. A, 112, 1981–1985, 2007.

Rimetz-Planchon, J., Dhooghe, F., Schoon, N., Vanhaecke, F., and Amelynck, C.: Chemical ionization by $[NO]^+$ and subsequent collision-induced dissociation for the selective on-line detection of monoterpenes and linalool, Rapid Commun. Mass Sp., 25, 647–654, 2011.

Roberts, J. M.: The atmospheric chemistry of organic nitrates, Atmos. Environ. A-Gen., 24, 243–287, 1990.

Roberts, J. M., Flocke, F., Stroud, C. A., Hereid, D., Williams, E., Fehsenfeld, F., Brune, W., Martinez, M., and Harder, H.: Ground-based measurements of peroxycarboxylic nitric anhydrides (PANs) during the 1999 Southern Oxidants Study Nashville Intensive, J. Geophys. Res.-Atmos., 107, 4554, doi:10.1029/2001JD000947, 2002.

Rollins, A. W., Fry, J. L., Hunter, J. F., Kroll, J. H., Worsnop, D. R., Singaram, S. W., and Cohen, R. C.: Elemental analysis of aerosol organic nitrates with electron ionization high-resolution mass spectrometry, Atmos. Meas. Tech., 3, 301–310, doi:10.5194/amt-3-301-2010, 2010.

Sadanaga, Y., Takaji, R., Ishiyama, A., Nakajima, K., Matsuki, A., and Bandow, H.: Thermal dissociation cavity attenuated phase shift spectroscopy for continuous measurement of total peroxy and organic nitrates in the clean atmosphere, Rev. Sci. Instrum., 87, 074102, doi:10.1063/1.4958167, 2016.

Schoon, N., Amelynck, C., Debie, E., Bultinck, P., and Arijs, E.: A selected ion flow tube study of the reactions of H_3O^+, NO^+ and O_2^+ with a series of C_5, C_6 and C_8 unsaturated biogenic alcohols, Int. J. Mass Spectrom., 263, 127–136, 2007.

Slusher, D. L., Huey, L. G., Tanner, D. J., Flocke, F. M., and Roberts, J. M.: A thermal dissociation–chemical ionization mass spectrometry (TD-CIMS) technique for the simultaneous measurement of peroxyacyl nitrates and dinitrogen pentoxide, J. Geophys. Res.-Atmos., 109, D19315, doi:10.1029/2004JD004670, 2004.

Smith, D. and Španěl, P.: Selected ion flow tube mass spectrometry (SIFT-MS) for on-line trace gas analysis, Mass Spectrom. Rev., 24, 661–700, 2005.

Smith, D., Wang, T., and Spanel, P.: Analysis of ketones by selected ion flow tube mass spectrometry, Rapid Commun. Mass Sp., 17, 2655–2660, 2003.

Smith, D., Sovová, K., and Španěl, P.: A selected ion flow tube study of the reactions of H_3O^+, NO^+ and O_2^+ with seven isomers of hexanol in support of SIFT-MS, Int. J. Mass Spectrom., 319–320, 25–30, 2012.

Smith, G.: Comparative analysis of tekmar 3000 and 3100 purge and trap sample concentrators: Performance evaluation between electroform nickel and Silcosteel-coated sample pathways, Tekmar, Mason, OH, USA, 2003.

Spanel, P. and Smith, D.: SIFT studies of the reactions of H_3O^+, NO^+ and O_2^+ with a series of alcohols, Int. J. Mass Spectrom., 167–168, 375–388, 1997.

Španěl, P. and Smith, D.: Selected ion flow tube studies of the reactions of H_3O^+, NO^+, and O_2^+ with several aromatic and aliphatic hydrocarbons, Int. J. Mass Spectrom., 181, 1–10, 1998.

Spittler, M.: Untersuchungen zur troposphärischen Oxidation von Limonen: Produktanalysen, Aerosolbildung und Photolyse von Produkten, PhD thesis, Department of Physical Chemistry, University of Wuppertal, Germany, 2001.

Tanimoto, H., Hirokawa, J., Kajii, Y., and Akimoto, H.: A new measurement technique of peroxyacetyl nitrate at parts per trillion by volume levels: Gas chromatography/negative ion chemical ionization mass spectrometry, J. Geophys. Res.-Atmos., 104, 21343–21354, 1999.

Teng, A. P., Crounse, J. D., Lee, L., St. Clair, J. M., Cohen, R. C., and Wennberg, P. O.: Hydroxy nitrate production in the OH-initiated oxidation of alkenes, Atmos. Chem. Phys., 15, 4297–4316, doi:10.5194/acp-15-4297-2015, 2015.

Tuazon, E. C., Alvarado, A., Aschmann, S. M., Atkinson, R., and Arey, J.: Products of the gas-phase reactions of 1,3-butadiene with OH and NO_3 radicals, Environ. Sci. Technol., 33, 3586–3595, 1999.

Tureček, F.: Proton affinity of peroxyacetyl nitrate. A computational study of topical proton affinities, J. Mass Spectrom., 35, 1351–1359, 2000.

Wang, T., Španěl, P., and Smith, D.: A selected ion flow tube study of the reactions of H_3O^+, NO^+ and O_2^+ with some phenols, phenyl alcohols and cyclic carbonyl compounds in support of SIFT-MS and PTR-MS, Int. J. Mass Spectrom., 239, 139–146, 2004.

Winer, A. M., Peters, J. W., Smith, J. P., and Pitts, J. N.: Response of commercial chemiluminescent nitric oxide-nitrogen dioxide analyzers to other nitrogen-containing compounds, Environ. Sci. Technol., 8, 1118–1121, 1974.

Xiong, F., McAvey, K. M., Pratt, K. A., Groff, C. J., Hostetler, M. A., Lipton, M. A., Starn, T. K., Seeley, J. V., Bertman, S. B., Teng, A. P., Crounse, J. D., Nguyen, T. B., Wennberg, P. O., Misztal, P. K., Goldstein, A. H., Guenther, A. B., Koss, A. R., Olson, K. F., de Gouw, J. A., Baumann, K., Edgerton, E. S., Feiner, P. A., Zhang, L., Miller, D. O., Brune, W. H., and Shepson, P. B.: Observation of isoprene hydroxynitrates in the southeastern United States and implications for the fate of NO_x, Atmos. Chem. Phys., 15, 11257–11272, doi:10.5194/acp-15-11257-2015, 2015.